PLOS ONE

RESEARCH ARTICLE

Optical coherence tomography for glaucoma diagnosis: An evidence based meta-analysis

Vinay Kansal[1], James J. Armstrong[2], Robert Pintwala[2], Cindy Hutnik[3,4]*

1 University of Saskatchewan, Department of Ophthalmology, Saskatoon, Canada, **2** Western University Canada, Faculty of Medicine, London, Canada, **3** Western University Canada, Department of Ophthalmology, London, Canada, **4** Ivey Eye Institute, St. Joseph's Hospital, London, Canada

* cindy.hutnik@sjhc.london.on.ca

Citation: Kansal V, Armstrong JJ, Pintwala R, Hutnik C (2018) Optical coherence tomography for glaucoma diagnosis: An evidence based meta-analysis. PLoS ONE 13(1): e0190621. https://doi.org/10.1371/journal.pone.0190621

Editor: Patrice E. Fort, University of Michigan, UNITED STATES

Received: June 30, 2017

Accepted: December 18, 2017

Published: January 4, 2018

Data Availability Statement: All relevant data are within the paper and its Supporting Information files.

Funding: The authors received no specific funding for this work.

Competing interests: The authors have declared that no competing interests exist.

Abstract

Purpose

Early detection, monitoring and understanding of changes in the retina are central to the diagnosis of glaucomatous optic neuropathy, and vital to reduce visual loss from this progressive condition. The main objective of this investigation was to compare glaucoma diagnostic accuracy of commercially available optical coherence tomography (OCT) devices (Zeiss Stratus, Zeiss Cirrus, Heidelberg Spectralis and Optovue RTVue, and Topcon 3D-OCT).

Patients

16,104 glaucomatous and 11,543 normal eyes reported in 150 studies.

Methods

Between Jan. 2017 and Feb 2017, MEDLINE®, EMBASE®, CINAHL®, Cochrane Library®, Web of Science®, and BIOSIS® were searched for studies assessing glaucoma diagnostic accuracy of the aforementioned OCT devices. Meta-analysis was performed pooling area under the receiver operating characteristic curve (AUROC) estimates for all devices, stratified by OCT type (RNFL, macula), and area imaged.

Results

150 studies with 16,104 glaucomatous and 11,543 normal control eyes were included. Key findings: AUROC of glaucoma diagnosis for RNFL average for all glaucoma patients was 0.897 (0.887–0.906, n = 16,782 patient eyes), for macula ganglion cell complex (GCC) was 0.885 (0.869–0.901, n = 4841 eyes), for macula ganglion cell inner plexiform layer (GCIPL) was 0.858 (0.835–0.880, n = 4211 eyes), and for total macular thickness was 0.795 (0.754–0.834, n = 1063 eyes).

Conclusion

The classification capability was similar across all 5 OCT devices. More diagnostically favorable AUROCs were demonstrated in patients with increased glaucoma severity. Diagnostic

accuracy of RNFL and segmented macular regions (GCIPL, GCC) scans were similar and higher than total macular thickness. This study provides a synthesis of contemporary evidence with features of robust inclusion criteria and large sample size. These findings may provide guidance to clinicians when navigating this rapidly evolving diagnostic area characterized by numerous options.

Introduction

Glaucoma is the leading cause of irreversible blindness worldwide[1]. As the population continues to age, and average life expectancies increase, the prevalence of this debilitating disease will grow. Glaucoma is one of the leading causes of blindness in working-age populations of industrialized nations, and is the most common cause of permanent vision loss in persons older than 40 years of age, after age-related macular degeneration[2–4].

Glaucoma is a multifactorial, chronic optic nerve neuropathy that is characterized by progressive loss of retinal ganglion cells (RGC), which leads to structural damage to the optic nerve head (ONH), retinal nerve fiber layer (RNFL), and consequent visual field defects[5]. Early diagnosis and treatment of glaucoma has been shown to reduce the rate of disease progression, and improve patients' quality of life[6]. The currently accepted gold standards for glaucoma diagnosis are optic disc assessment for structural changes, and achromatic white-on-white perimetry to monitor changes in function[7]. However, imaging technologies such as optic coherence technology (OCT) are playing an increasing role in glaucoma diagnosis, monitoring of disease progress, and quantification of structural damage[8,9].

OCT is a non-invasive, non-contact imaging modality that provides high-resolution cross-sectional imaging of ocular tissues (retina, optic nerve, and anterior segment). Image acquisition is analogous to ultrasound, where light waves is used in lieu of sound waves. Low coherence infrared light is directed toward the tissue being imaged, from which it scatters at large angles. An interferometer (beam splitter) is used to record the path of scattered photons and create three-dimensional images[10–13]. OCT is highly reproducible, and is thus widely used as an adjunct in routine glaucoma patient management[14–16].

Peripapillary RNFL analysis is the most commonly used scanning protocol for glaucoma diagnosis[14–16], as it samples RGCs from the entire retina; however, it does suffer certain drawbacks related to inter-patient variability in ONH morphology[17,18]. To overcome some of these disadvantages, the macular thickness has been proposed as a means of glaucoma detection[19]– 50% of RGCs are found in the macula, and RGC bodies are thicker than their axons, thus are potentially easier to detect. The older time-domain (TD) OCT devices, such as Zeiss Stratus, were able to only measure total macular thickness, which had been shown to have poorer glaucoma diagnostic accuracy than RNFL thickness[20–22]. Spectral-domain (SD) OCT (Zeiss Cirrus, Heidelberg Spectralis, Optovue RTVue, Topcon 3D-OCT) allows for measurement of specific retinal layers implicated in the pathogenesis of glaucoma, namely: macular nerve fiber layer (mNFL), ganglion cell layer with inner plexiform layer (GCIPL), and ganglion cell complex (GCC) (composed of mNFL and GCIPL). Segmented analysis is purported to have better diagnostic ability for glaucoma than total retinal thickness[23,24], and may be comparable to RNFL thickness[23,25,26].

Currently, several OCT devices are available on the market, each with unique technologies purported to provide better clinical information to the user. The technical features of these various systems have been described elsewhere[27,28]. Reichel et al. also provide images obtained

from each of the OCT systems[27]. It is unclear however; which OCT device should be selected by practitioners when making referral or treatment decisions. The aim of this meta-analysis was to provide pooled estimates for the accuracy and detection capability of the most commonly used OCT imaging devices (Zeiss Cirrus OCT, Zeiss, Stratus OCT, Heidelberg Spectralis, Optovue RTVue, Topcon 3D-OCT) for glaucoma diagnosis and classification between patients and healthy individuals.

Methods

Overview of review methods

The main objective of this investigation was to compare the glaucoma diagnostic accuracy for each of the OCT devices commercially available, namely Zeiss Stratus, Zeiss Cirrus, Heidelberg Spectralis, Optovue RTVue and Topcon 3D-OCT. We compared diagnostic accuracies of RNFL and macular parameters obtained by these imaging devices. This review was performed in accordance with the Preferred Reporting Items for Systematic Reviews and Meta-Analyses (PRISMA) statement methodology[29]. A PRISMA flow diagram is used to illustrate the flow of records throughout this review (Fig 1).

Data sources and search strategy

The search strategy for this investigation was comprehensive, aiming to retrieve the largest possible number of relevant studies. An electronic search strategy was developed through consultation with an experienced ophthalmologist specializing in glaucoma management. The search end date was February 2017. There was no specified search start date. Any study providing information on area under receiver operating characteristic curve, sensitivity, specificity, negative predictive value, positive predictive value, likelihood ratio, or diagnostic odds ratio was included. Published and unpublished studies were considered.

The following bibliographic databases were searched: MEDLINE® (Ovid MEDLINE(R) Epub Ahead of Print, In-Process & Other Non-Indexed Citations, Ovid MEDLINE(R) Daily, Ovid MEDLINE and Versions(R)), EMBASE® (Embase Classic+Embase), CINAHL®, Cochrane Library® (Wiley Library), Web of Science®, and BIOSIS®. Specific keywords used in the search included terms for glaucoma, optical coherence tomography, imaging device manufacturer (ie. Zeiss, Heidelberg, RTVue, Topcon), and diagnostic testing including terms for diagnostic evaluative tests (ie. Area under receiver operating characteristic curve, etc.). Search strategies for each of the devices are available in S1 Table (Appendix 1).

Inclusion and exclusion criteria

All studies that assessed the diagnostic accuracy of OCT for detection of glaucoma were considered for inclusion in our review. As the goal of this investigation was to maximize generalizability and applicability to clinical practice, a broad gold standard was accepted for inclusion, ie. White on white automated perimetry, optic disc appearance (clinically or by photograph), or combination thereof. Accepting a wider gold standard more accurately reflects the reality of clinical practice, and allowed for inclusion of a larger number of articles, improving robustness of the quantitative meta-analysis. Only human, clinical studies published in English-language were accepted. Patient were 18 years of age or greater. No exclusions were made for patient ethnicity, or country where study was conducted. Included studies assessed at least one of five devices, namely Stratus OCT (Carl Zeiss Meditec, Jena, Germany), Cirrus OCT (Carl Zeiss Meditec), Spectralis OCT (Heidelberg Engineering Inc., Heidelberg, Deutschland), RTVue (Optovue Inc., Freemont, United States), and 3D-OCT (Topcon, Tokyo, Japan). These devices

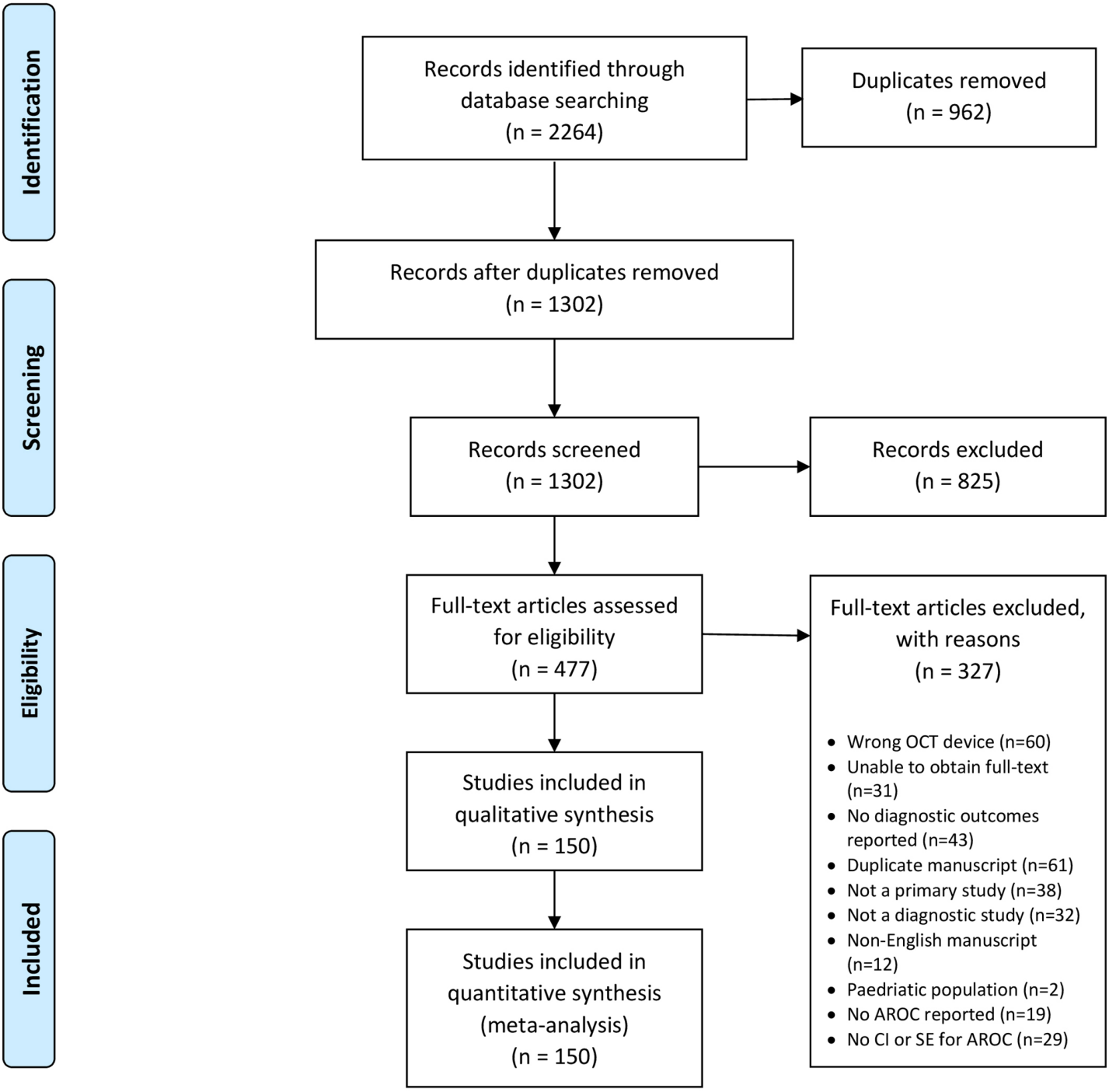

Fig 1. Study flow in this meta-analysis (PRISMA guidelines).

https://doi.org/10.1371/journal.pone.0190621.g001

were included as they represent the newest or most widely utilized OCT devices available for glaucoma diagnosis at the time of this review. Studies of both RNFL and macular areas for glaucoma diagnosis were included.

During full-text screening, articles were included if they reported area under receiver operating characteristic curve (AUROC) statistics. Manuscripts that did not report standard error

or confidence intervals for AUROC were excluded. Other exclusions were: duplicate manuscripts, non-diagnostic studies, studies of pediatric patients, studies without control participants, and investigations of OCT devices other than those previously specified.

Study selection

All studies included for consideration underwent two levels of screening by two independent reviewers. All records were uploaded to an online interface (Covidence, Veritas Health Innovation, Melbourne, Australia) to coordinate and support the screening process. First, a broad screen of titles, keywords and abstracts (Level 1) was performed. At this stage, studies were tagged as either "Relevant", "Irrelevant" or "Maybe Relevant". For all relevant studies, full text screening was performed (Level 2) using the stricter *a priori* inclusion criteria detailed previously.

After each level of screening, disagreements between article screeners were resolved through consultation with the primary author. Reasons for exclusion were documented and are reported in the review. The PRISMA flow chart of studies during screening is illustrated in Fig 1.

Data extraction and quality assessment

An electronic data extraction form specific to this meta-analysis was developed *a priori*. Data collected included study identification information (title, authors, journal and year of publication, study methodology (design, inclusion/exclusion criteria, gold standard type), patient variables (number of patients/controls, glaucoma diagnosis, age, gender), OCT device used, area imaged (RNFL, macula subtype), and AUROC (with SE/CI).

The quality assessment of diagnostic accuracy studies, version 2 (QUADAS-2)[30] was used to assess the risk of bias and applicability concerns of all manuscripts included in this review. This assessment tool comprises four key domains: 1) patient selection, 2) index test, 3) reference standard, and 4) flow of patients through the study and timing between index test and reference standard. Each domain was assessed in terms of risk of bias. The first three domains were assessed for their applicability to the research question being assessed by the review. Results of QUADAS-2 are summarized in Fig 2.

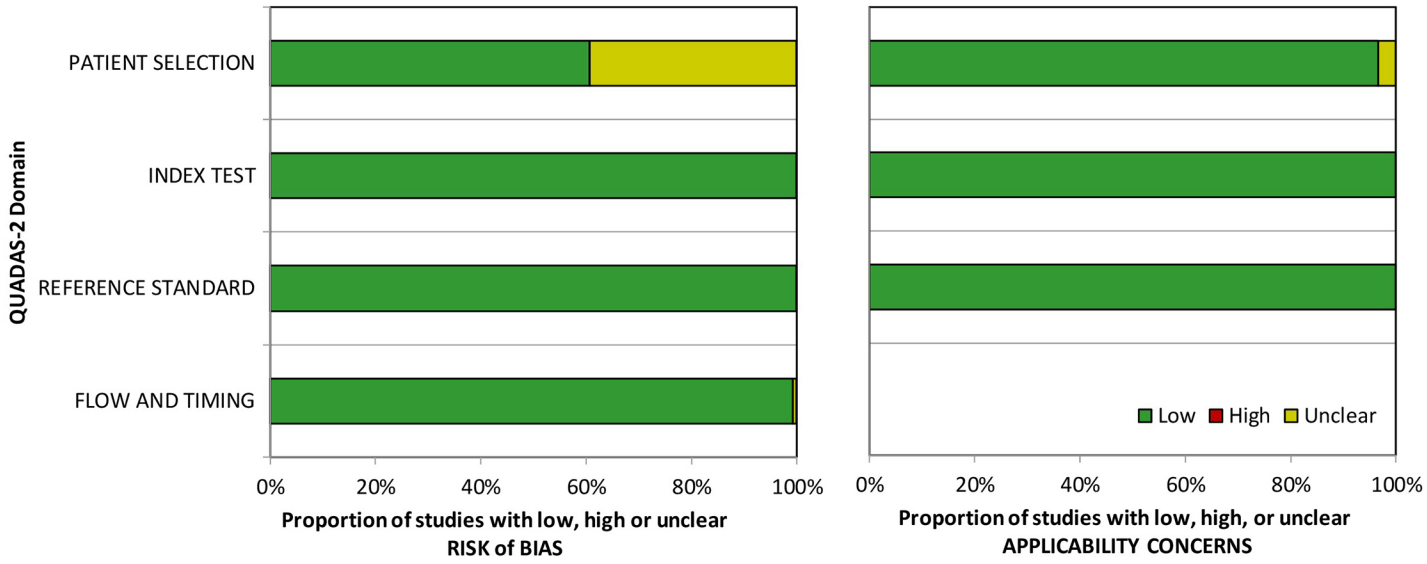

Fig 2. Methodological quality of included studies using the QUADAS 2 tool.

https://doi.org/10.1371/journal.pone.0190621.g002

Data synthesis and statistical analysis

All statistical analyses were performed using MedCalc (Version 17.2, MedCalc Software, Ostend, Belgium). Meta-analysis for the AUROC was selected instead of other measures such as sensitivity and specificity. The AUROC is a commonly used metric for diagnostic accuracy of medical tests. It was found to be more consistently reported in the included studies. Whereas some studies reported a combination of parameters, others reported sensitivity values for particular specificity cut-offs, which, in turn, were not consistent across studies. AUROC reflects both the sensitivity and specificity of a diagnostic test, can be compared across studies, and can be combined between similar studies when measures of uncertainty (standard error (SE) or confidence interval (CI)) are provided[31].

Meta-analysis was completed using MedCalc (MedCalc, Version 17.2, MedCalc Software, Ostend, Belgium). The main outcome of this study was pooled AUROC for each of the following groups: all glaucoma patients, perimetric glaucoma, pre-perimetric, mild glaucoma, moderate to severe glaucoma, and myopic glaucoma. As there currently does not exist any international consensus on the definition of glaucoma severity, there was heterogeneity in the way that each study defined their patient groups. For consistency, we defined each group as follows: 1) *Perimetric glaucoma*–glaucoma based on abnormal visual field measurements; 2) *Pre-perimetric glaucoma*–glaucoma diagnosed based on optic disc appearance, with normal visual field measurements; 3) *Mild glaucoma*–perimetric glaucoma, defined as mean deviation of $>$ -6.00 dB as per the Hodapp-Parrish-Anderson criteria[32]. Patients with normal visual fields were not included in this group; 4) *Moderate to severe glaucoma*–perimetric glaucoma, defined as mean deviation $<$ -6.00 dB[32]; 5) *Myopic glaucoma*–any definition of myopia as defined by study authors, this could include dioptric definition (ex. Spherical equivalent $<$ -6.0) or axial length definition (AL $>$25mm).

Individual measures of AUROC from each study were pooled into a weighted summary AUROC for each group using the methods described in Zhou et al.[31] Heterogeneity among included studies was tested by computing the I^2, Z-value and $\chi 2$ statistics. An I^2 value of less than 50% implies low heterogeneity and supports the use of a fixed-effect meta-analysis model. A value of greater than or equal to 50% implies high heterogeneity and supports the use of a random-effects model. Additionally, a high Z-value, a low p-value ($<$0.01) and a large $\chi 2$ value implies significant heterogeneity and supports the use of a random-effects model using DerSimonian and Laird methods. Forest plots were generated to visualize results. Publication bias was assessed through evaluation of funnels plots of included studies for each pooled AUROC.

Results

Search results and study characteristics

Study flow is summarized in Fig 1. After removal of duplicates, 1301 records underwent title and abstract (Level 1) screening. 825 were excluded as irrelevant. The remaining 477 records underwent full-text screening (Level 2). Of these, 327 articles were excluded as they did not meet the study inclusion criteria, or manuscript was unable to be obtained. At the end of screening, 150 articles were included for meta-analysis [21–24,33–178].

Characteristics of the 150 included studies are presented in S2 Table (Appendix 2). 67 (44.7%) of studies were case-control studies, 73 (48.7%) were cross-sectional studies, and 10 (6.7%) were cohort studies. 34 (22.7%) used visual field as a reference standard, 6 (4.0%) used disc appearance, 110 (73.3%) used a combination of structural and functional criteria. 55 studies examined the Zeiss Cirrus OCT, 49 studies assessed Zeiss Stratus OCT, 23 studies evaluated Heidelberg Spectralis, 38 studies examined Optovue RTVue, and 14 studies evaluated the

Table 1. Summarized study and patient characteristics.

				Gender	
	# of eyes	# of Studies	Age ± SD (# of study groups, # of studies)	Male (%) (# of study groups, # of studies)	Female (%) (# of study groups, # of studies)
Patient groups					
Normal Controls	11543	150	54.1 ± 11.1 (141,141)	3683 (46.5%) (109,109)	4232 (53.5%) (109,109)
All Glaucoma Patients	16103	150	58.8 ± 11.2 (214,137)	5255 (49.3%) (158,103)	5403 (50.7%) (158,103)
Perimetric (severity unspecified)	10335	122	60.1 ± 11.3 (108,96)	3196 (49.6%) (77,70)	3248 (50.4%) (77,70)
Preperimetric	1711	39	56.4 ± 10.7 (32,29)	502 (42.7%) (23,22)	673 (57.3%) (23,22)
Mild	2369	40	57 ± 11.3 (35,30)	829 (50.2%) (28,23)	823 (49.8%) (28,23)
Moderate to Severe	1199	24	60.4 ± 11.4 (18,10)	325 (51.2%) (15,8)	310 (48.8%) (15,8)
Myopic	358	9	45.3 ± 10.6 (8,7)	194 (58.8%) (7,7)	136 (41.2%) (7,7)
OCT Device					
Cirrus	7362	53	57.4 ± 11.9 (75,49)	2249 (49.7%) (50,36)	2273 (50.3%) (50,36)
Stratus	3120	42	58.9 ± 10.2 (47,37)	1083 (48.7%) (37,28)	1141 (51.3%) (37,28)
Spectralis	1710	20	62.7 ± 10.5 (25,20)	668 (52.4%) (20,16)	606 (47.6%) (20,16)
RTVue	3048	30	59.5 ± 11.1 (47,26)	993 (47%) (41,20)	1119 (53%) (41,20)
3D-Topcon	863	10	59.7 ± 11.5 (15,10)	262 (49.8%) (9,6)	264 (50.2%) (9,6)
Imaged Regions					
RNFL	13089	130	58.7 ± 11.2 (162,117)	4213 (49.8%) (117,87)	4245 (50.2%) (117,87)
Macula–GCIPL	1217	6	59.9 ± 12.9 (13,5)	331 (52.9%) (8,4)	295 (47.1%) (8,4)
Macula–GCC	1075	9	59.7 ± 10.9 (17,8)	392 (42.3%) (17,8)	535 (57.7%) (17,8)
Macula—mNFL	237	3	58.6 ± 11.8 (5,3)	84 (42.2%) (4,2)	115 (57.8%) (4,2)
Macula–Total thickness	485	7	58.1 ± 8.9 (12,7)	235 (52.5%) (11,5)	213 (47.5%) (11,5)

https://doi.org/10.1371/journal.pone.0190621.t001

Topcon 3D-OCT. There were 50.0% male, and 50.0% female glaucoma patients (reported in 150 studies). Controls were 46.5% male, 53.5% female (reported in 109 studies). The mean age of glaucoma patients was 58.8 ± 11.2, of controls was 54.1 ± 11.1 (Table 1).

Study quality

A summary of the methodological quality assessment for included studies is provided in Fig 2. Overall methodological quality of all included studies was strong in terms of risk of bias and applicability to the research question. Of note, there was an unclear risk of bias in patient selection for 39.3% of studies. This was largely due to inadequate reporting of patient selection methods in these manuscripts; thus, risk of bias was unable to be ascertained.

Diagnostic accuracy of OCT for all glaucoma patients, RNFL and macular parameters

The diagnostic accuracy of OCT for all glaucoma patients stratified by imaged area and device is reported in Table 2, and displayed graphically in Fig 3. Pooled AUROC ranged from 0.632 to 0.915 depending on imaging device and area imaged. Overall, there were no statistically significance differences between devices for any particular area imaged. Within RNFL parameters, we found that AUROC for glaucoma diagnosis was higher for average (0.897, CI95% 0.887 to 0.906), superior (0.855, CI95% 0.844 to 0.866) and inferior (0.895, CI95% 0.886 to 0.905) areas than nasal (0.707, CI95% 0.692 to 0.721) and temporal (0.742, CI95% 0.727 to 0.757) parameters. For the Macular GCIPL scans, average (0.858, CI95% 0.835 to 0.880), inferior (0.860, CI95% 0.840 to 0.880), temporal (superotemporal (0.825, CI95% 0.796 to 0.854),

Table 2. Pooled AUROCs of RNFL and macular OCT parameters for all glaucoma patients.

All Glaucoma Patients–Pooled AUROCs (if I^2 > 50% random effects meta-analysis was used, if I^2 < 50% fixed effects was used)											
Test Parameter, Location and OCT Device	**Number of Studies**	**Number of Study Groups***	**Pooled Sample Size (controls)**	**Pooled AUROC**	**95% CI**	**Test Parameter, Location and OCT Device**	**Number of Studies**	**Number of Study Groups***	**Pooled Sample Size (eyes)**	**Pooled AUROC**	**95% CI**
RNFL						**Macula—GCIPL**					
Average	*135*	*236*	*16,782 (18,490)*	*0.897*	*0.887 to 0.906*	Average	28	50	4,211 (4,401)	0.858	0.835 to 0.880
Cirrus	*52*	*82*	*6,924 (8,569)*	*0.915*	*0.903 to 0.927*	*Cirrus*	*22*	*34*	*3062 (3483)*	*0.877*	*0.854 to 0.900*
Stratus	*43*	*56*	*3,447 (3746)*	*0.886*	*0.865 to 0.907*	*Topcon*	*9*	*15*	*1072 (859)*	*0.805*	*0.760 to 0.850*
Spectralis	*19*	*28*	*1682 (1988)*	*0.898*	*0.872 to 0.923*	Inferior	26	54	4,106 (4,428)	0.860	0.840 to 0.880
RTVue	*36*	*52*	*3540 (3255)*	*0.886*	*0.866 to 0.907*	*Cirrus*	*21*	*36*	*2950 (3381)*	*0.876*	*0.852 to 0.900*
Topcon	*12*	*18*	*1189 (932)*	*0.879*	*0.841 to 0.917*	*Spectralis*	*1*	*2*	*120 (120)*	*0.841*	*0.791 to 0.890*
Inferior	*103*	*183*	*13,265 (14,580)*	*0.895*	*0.886 to 0.905*	*Topcon*	*9*	*16*	*1036 (927)*	*0.821*	*0.777 to 0.866*
Cirrus	*45*	*69*	*5701 (6862)*	*0.908*	*0.894 to 0.922*	Superior	26	53	4,038 (4,364)	0.797	0.775 to 0.820
Stratus	*34*	*43*	*2701 (3101)*	*0.886*	*0.863 to 0.909*	*Cirrus*	*21*	*36*	*2950 (3381)*	*0.816*	*0.790 to 0.842*
Spectralis	*10*	*16*	*920 (1045)*	*0.925*	*0.909 to 0.941*	*Spectralis*	*1*	*2*	*120 (120)*	*0.697*	*0.629 to 0.765*
RTVue	*30*	*39*	*2941 (2707)*	*0.875*	*0.854 to 0.896*	*Topcon*	*9*	*15*	*968 (863)*	*0.757*	*0.714 to 0.800*
Topcon	*10*	*16*	*1002 (865)*	*0.884*	*0.851 to 0.917*	Superotemporal	18	30	2,315 (2,336)	0.825	0.796 to 0.854
Superior	*100*	*178*	*12,873 (14,207)*	*0.855*	*0.844 to 0.866*	*Cirrus*	*17*	*27*	*2,064 (2,195)*	*0.831*	*0.801 to 0.861*
Cirrus	*44*	*66*	*5505 (6698)*	*0.881*	*0.866 to 0.895*	*Topcon*	*1*	*2*	*174 (82)*	*0.690*	*0.573 to 0.807*
Stratus	*34*	*43*	*2701 (3101)*	*0.832*	*0.807 to 0.858*	Superonasal	18	30	2,315 (2,336)	0.757	0.722 to 0.792
Spectralis	*9*	*15*	*887 (1013)*	*0.872*	*0.843 to 0.901*	*Cirrus*	*17*	*27*	*2,064 (2,195)*	*0.762*	*0.725 to 0.799*
RTVue	*29*	*38*	*2778 (2530)*	*0.834*	*0.809 to 0.858*	*Topcon*	*1*	*2*	*174 (82)*	*0.648*	*0.511 to 0.784*

(*Continued*)

Table 2. (*Continued*)

All Glaucoma Patients–Pooled AUROCs (if I^2 > 50% random effects meta-analysis was used, if I^2 < 50% fixed effects was used)											
Test Parameter, Location and OCT Device	**Number of Studies**	**Number of Study Groups***	**Pooled Sample Size (controls)**	**Pooled AUROC**	**95% CI**	**Test Parameter, Location and OCT Device**	**Number of Studies**	**Number of Study Groups***	**Pooled Sample Size (eyes)**	**Pooled AUROC**	**95% CI**
Topcon	*10*	*16*	*1002 (865)*	*0.843*	*0.806 to 0.880*	Inferotemporal	18	30	2,315 (2,336)	0.877	0.853 to 0.902
Nasal	*82*	*147*	*10,409 (10,838)*	*0.707*	*0.692 to 0.721*	*Cirrus*	*17*	*27*	*2,064 (2,195)*	*0.879*	*0.853 to 0.904*
Cirrus	*38*	*58*	*4719 (4806)*	*0.678*	*0.656 to 0.701*	*Topcon*	*1*	*2*	*174 (82)*	*0.793*	*0.704 to 0.882*
Stratus	*32*	*41*	*2501 (2860)*	*0.734*	*0.708 to 0.759*	Inferonasal	18	30	2,315 (2,336)	0.783	0.754 to 0.812
Spectralis	*13*	*19*	*1127 (1322)*	*0.737*	*0.701 to 0.773*	*Cirrus*	*17*	*27*	*2,064 (2,195)*	*0.789*	*0.760 to 0.819*
RTVue	*16*	*18*	*1268 (1215)*	*0.761*	*0.729 to 0.793*	*Topcon*	*1*	*2*	*174 (82)*	*0.632*	*0.515 to 0.750*
Topcon	*7*	*11*	*794 (635)*	*0.639*	*0.613 to 0.665*	Minimum					
Temporal	*84*	*149*	*10,616 (10,969)*	*0.742*	*0.727 to 0.757*	*Cirrus*	16	24	1,948 (2,054)	0.898	0.870 to 0.925
Cirrus	*38*	*58*	*4719 (4806)*	*0.747*	*0.723 to 0.771*						
Stratus	*33*	*42*	*2562 (2917)*	*0.722*	*0.694 to 0.750*	**Macula–Total Thickness**					
Spectralis	*13*	*19*	*1127 (1322)*	*0.748*	*0.708 to 0.788*	Average	11	20	1,063 (816)	0.794	0.754 to 0.834
RTVue	*17*	*19*	*1414 (1289)*	*0.772*	*0.728 to 0.817*	*Cirrus*	*1*	*2*	*96 (70)*	*0.842*	*0.772 to 0.913*
Topcon	*7*	*11*	*794 (635)*	*0.723*	*0.668 to 0.777*	*Stratus*	*5*	*8*	*359 (354)*	*0.769*	*0.697 to 0.840*
						Spectralis	*2*	*2*	*140 (73)*	*0.797*	*0.717 to 0.876*
Macula—GCC						*RTVue*	*3*	*7*	*438 (284)*	*0.825*	*0.768 to 0.883*
Average	*39*	*70*	*4,841 (4,103)*	*0.885*	*0.869 to 0.901*						
Cirrus	*6*	*9*	*675 (495)*	*0.873*	*0.837 to 0.908*						

(*Continued*)

Table 2. (*Continued*)

All Glaucoma Patients–Pooled AUROCs (if I^2 > 50% random effects meta-analysis was used, if I^2 < 50% fixed effects was used)											
Test Parameter, Location and OCT Device	**Number of Studies**	**Number of Study Groups***	**Pooled Sample Size (controls)**	**Pooled AUROC**	**95% CI**	**Test Parameter, Location and OCT Device**	**Number of Studies**	**Number of Study Groups***	**Pooled Sample Size (eyes)**	**Pooled AUROC**	**95% CI**
RTVue	*29*	*45*	*3161 (2799)*	*0.886*	*0.865 to 0.906*						
Topcon	*10*	*15*	*928 (750)*	*0.890*	*0.853 to 0.926*						
Inferior	*31*	*52*	*3,689 (3,155)*	*0.876*	*0.858 to 0.893*						
Cirrus	*4*	*6*	*530 (363)*	*0.893*	*0.861 to 0.924*						
RTVue	*24*	*31*	*2231 (2042)*	*0.874*	*0.852 to 0.896*						
Topcon	*10*	*15*	*928 (750)*	*0.880*	*0.844 to 0.916*						
Superior	*31*	*52*	*3689 (3155)*	*0.812*	*0.790 to 0.834*						
Cirrus	*4*	*6*	*530 (363)*	*0.811*	*0.752 to 0.869*						
RTVue	*24*	*31*	*2231 (2042)*	*0.814*	*0.786 to 0.842*						
Topcon	*10*	*15*	*928 (750)*	*0.808*	*0.766 to 0.851*						
Focal Loss Volume											
RTVue	*18*	*28*	*1745 (1797)*	*0.885*	*0.864 to 0.905*						
Global Loss Volume											
RTVue	*19*	*28*	*2296 (2194)*	*0.868*	*0.842 to 0.895*						

*Certain studies reported outcomes of several glaucoma subgroups.

https://doi.org/10.1371/journal.pone.0190621.t002

inferotemporal (0.877, CI95% 0.853 to 0.902)) and minimum parameters had higher AUROC for glaucoma diagnosis than nasal (superonasal (0.757, CI95% 0.722 to 0.792, inferonasal (0.783, CI95% 0.754 to 0.812)) areas. By comparison, there were no major differences between areas for the macular GCC scans.

Comparing the diagnostic efficacy between RNFL and macular thickness, we note that average RNFL (0.897, CI95% 0.887 to 0.906), average macula GCC (0.885, CI95% 0.869 to 0.901), and average macula GCIPL (0.858, CI95% 0.835 to 0.880) thicknesses have similar AUROC

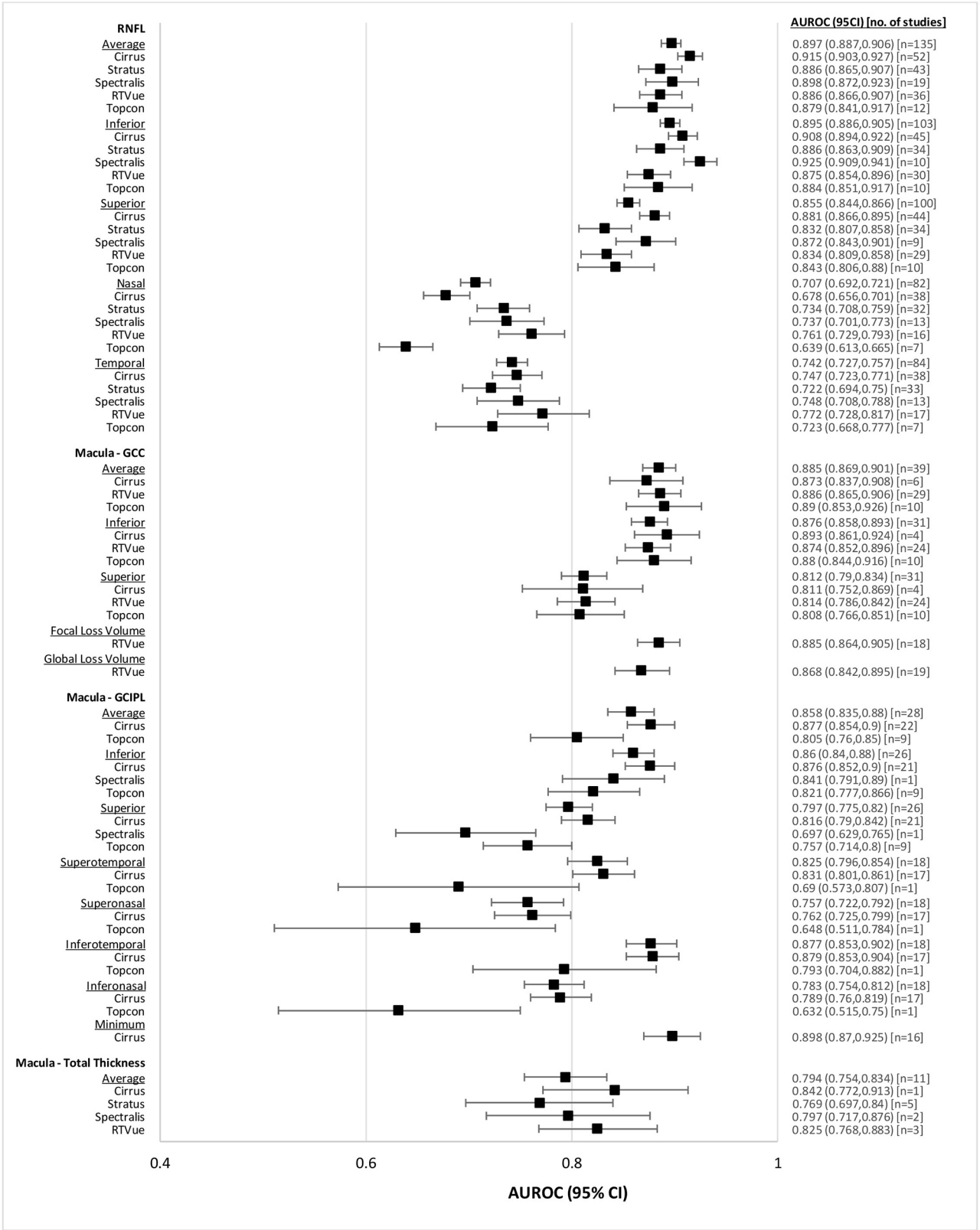

Fig 3. Forest plot of diagnostic accuracies of RNFL and macular OCT parameters, all glaucoma patients.

https://doi.org/10.1371/journal.pone.0190621.g003

for glaucoma diagnosis. By comparison, AUROC of average macular total thickness (0.794, CI95% 0.754 to 0.834) is lower.

Diagnostic accuracy of OCT for patient subgroups, RNFL and macular parameters

Perimetric glaucoma. Diagnostic accuracy of OCT for patients with perimetric glaucoma is reported in Table 3, and represented in a forest plot in Fig 4. Findings largely mirror what was found for the overall glaucoma population, with AUROCs being higher. All devices performed relatively similarly for glaucoma diagnosis, with the Zeiss Cirrus OCT demonstrating highest AUROC for most RNFL and Macula GCIPL parameters. For the RNFL, average (0.905, CI95% 0.895 to 0.916), superior (0.870, CI95% 0.858 to 0.883), and inferior (0.907, CI95% 0.897 to 0.918) thicknesses had higher AUROC than nasal (0.730, CI95% 0.712 to 0.748) and temporal (0.760, CI95% 0.742 to 0.778) regions. Within macula GCIPL, the Macular GCIPL scans, average (0.864, CI95% 0.837 to 0.890), inferior (0.861, CI95% 0.836 to 0.886), temporal (superotemporal (0.835, CI95% 0.792 to 0.877), inferotemporal (0.879, CI95% 0.848 to 0.910)) and minimum (0.904, CI95% 0.875 to 0.933) parameters had higher AUROC for glaucoma diagnosis than nasal (superonasal (0.778, CI95% 0.727 to 0.829), inferonasal (0.789, CI95% 0.752 to 0.827)) areas. There were no notable differences in AUROC between different macular GCC areas.

Average RNFL (0.905, CI95% 0.895 to 0.916), average macular GCIPL (0.864, CI95% 0.837 to 0.890), average macular GCC (0.895, CI95% 0.874 to 0.916) performed similarly well for glaucoma diagnosis. Conversely, average macular mNFL (0.799, CI95% 0.742 to 0.857) and average total macular thickness (0.792, CI95% 0.744 to 0.840) had lower AUROC. Across OCT devices, no major differences were noted for any of the parameters.

Pre-perimetric glaucoma. Pooled AUROCs for pre-perimetric glaucoma patients are reported in Table 4, and illustrated in a forest plot (Fig 5). There were no major differences across devices for any of the RNFL or macular parameters. Across RNFL parameters, average (0.831, CI95% 0.808 to 0.854), inferior (0.828, CI95% 0.801 to 0.855) and superior (0.774, CI95% 0.740 to 0.809) had larger AUROC than nasal (0.645, CI95% 0.610 to 0.680) or temporal (0.667, CI95% 0.627 to 0.707). All parameters within both macula GCIPL and macula GCC scans performed similarly well.

Overall, average RNFL (0.831, CI95% 0.808 to 0.854) had higher AUROC for glaucoma diagnosis than both average macula GCIPL (0.762, CI95% 0.708 to 0.816) and average macula GCC (0.797, CI95% 0.768 to 0.825).

Mild glaucoma. The diagnostic capability of OCT for patients with mild glaucoma is summarized in Table 5, and illustrated in Fig 6. RTVue OCT demonstrated a smaller AUROC than the other reviewed OCT devices for RNFL average (0.847, CI95% 0.781 to 0.913), inferior (0.826, CI95% 0.763 to 0.890), and superior parameters (0.784, CI95% 0.725 to 0.843). Across RNFL parameters, again average (0.912, CI95% 0.892 to 0.932), superior (0.860, CI95% 0.834 to 0.865) and inferior (0.901, CI95% 0.881 to 0.921) areas have higher diagnostic value than nasal (0.700, CI95% 0.667 to 0.732) and temporal (0.732, CI95% 0.698 to 0.766) regions. For macular GCC scans, all areas performed similarly well. Overall, RNFL parameters had higher AUROC than macular GCC (average RNFL (0.912, CI95% 0.892 to 0.932), average macular GCC (0.861, CI95% 0.819 to 0.903)).

Moderate to severe glaucoma. AUROCs of OCT for patients with moderate to severe glaucoma are summarized in Table 6, and illustrated in Fig 7. Overall, all OCT devices performed similarly well for glaucoma diagnosis. All RNFL parameters reported—average (0.959, CI95% 0.946 to 0.972), superior (0.923, CI95% 0.905 to 0.941) and inferior (0.954, CI95%

Table 3. Pooled AUROCs of RNFL and macular OCT parameters for perimetric glaucoma patients.

Perimetric Glaucoma–Pooled AUROCs (if I^2 > 50% random effects meta-analysis was used, if I^2 < 50% fixed effects was used)									
Test Parameter, Location and OCT Device	**Number of Studies**	**Pooled Sample Size**	**Pooled AUROC**	**95% CI**	**Test Parameter, Location and OCT Device**	**Number of Studies**	**Pooled Sample Size**	**Pooled AUROC**	**95% CI**
RNFL					**Macula–GCC**				
Average	123	10612 (9938)	0.905	0.895 to 0.916	Average	28	2599 (1799)	0.895	0.874 to 0.916
Cirrus	*43*	*4310 (4472)*	*0.924*	*0.911 to 0.936*	*Cirrus*	*4*	*347 (209)*	*0.887*	*0.853 to 0.922*
Stratus	*34*	*2498 (2416)*	*0.897*	*0.875 to 0.918*	*RTVue*	*18*	*1742 (1237)*	*0.898*	*0.869 to 0.927*
Spectralis	*14*	*1023 (944)*	*0.906*	*0.874 to 0.938*	*Topcon*	*5*	*433 (294)*	*0.894*	*0.867 to 0.920*
RTVue	*25*	*2161 (1745)*	*0.901*	*0.877 to 0.925*	Inferior	20	1867 (1280)	0.883	0.857 to 0.909
Topcon	*7*	*620 (361)*	*0.855*	*0.792 to 0.918*	*Cirrus*	*2*	*251 (128)*	*0.855*	*0.724 to 0.987*
Inferior	97	8352 (7892)	0.907	0.897 to 0.918	*RTVue*	*13*	*1183 (858)*	*0.884*	*0.848 to 0.920*
Cirrus	*36*	*3461 (3458)*	*0.916*	*0.900 to 0.933*	*Topcon*	*5*	*433 (294)*	*0.880*	*0.851 to 0.909*
Stratus	*27*	*1932 (2027)*	*0.910*	*0.889 to 0.931*	Superior	20	1867 (1280)	0.817	0.784 to 0.851
Spectralis	*9*	*645 (603)*	*0.915*	*0.883 to 0.946*	*Cirrus*	*2*	*251 (128)*	*0.793*	*0.732 to 0.854*
RTVue	*20*	*1881 (1510)*	*0.928*	*0.919 to 0.938*	*RTVue*	*13*	*1183 (858)*	*0.829*	*0.784 to 0.874*
Topcon	*5*	*433 (294)*	*0.875*	*0.818 to 0.932*	*Topcon*	*5*	*433 (294)*	*0.799*	*0.765 to 0.833*
Superior	94	8108 (7648)	0.870	0.858 to 0.883	Focal Loss Volume				
Cirrus	*35*	*3413 (3423)*	*0.889*	*0.872 to 0.907*	RTVue	10	836 (663)	0.874	0.832 to 0.916
Stratus	*27*	*1932 (2027)*	*0.856*	*0.833 to 0.879*	Global Loss Volume				
Spectralis	*8*	*612 (571)*	*0.883*	*0.844 to 0.922*	RTVue	12	1145 (914)	0.893	0.858 to 0.928
RTVue	*19*	*1718 (1333)*	*0.856*	*0.823 to 0.889*	**Macula–mNFL**				
Topcon	*5*	*433 (294)*	*0.850*	*0.804 to 0.897*	Average				
Nasal	82	6722 (6255)	0.730	0.712 to 0.748	Cirrus	2	140 (158)	0.799	0.742 to 0.857
Cirrus	*30*	*2857 (2596)*	*0.703*	*0.675 to 0.731*	**Macula–Total Thickness**				
Stratus	*25*	*1732 (1786)*	*0.754*	*0.729 to 0.778*	Average	10	688 (440)	0.792	0.744 to 0.840
Spectralis	*11*	*806 (758)*	*0.768*	*0.724 to 0.813*	*Stratus*	*5*	*261 (238)*	*0.781*	*0.734 to 0.829*
RTVue	*11*	*894 (821)*	*0.762*	*0.714 to 0.810*	*RTVue*	*3*	*289 (144)*	*0.777*	*0.656 to 0.898*
Topcon	*5*	*433 (294)*	*0.612*	*0.548 to 0.676*	Superior Outer				
Temporal	84	6929 (6386)	0.760	0.742 to 0.778	Stratus	4	791 (765)	0.767	0.732 to 0.803

(*Continued*)

Table 3. (*Continued*)

Perimetric Glaucoma–Pooled AUROCs (if I^2 > 50% random effects meta-analysis was used, if I^2 < 50% fixed effects was used)									
Test Parameter, Location and OCT Device	**Number of Studies**	**Pooled Sample Size**	**Pooled AUROC**	**95% CI**	**Test Parameter, Location and OCT Device**	**Number of Studies**	**Pooled Sample Size**	**Pooled AUROC**	**95% CI**
Cirrus	*30*	*2857 (2596)*	*0.759*	*0.729 to 0.790*	Inferior Outer				
Stratus	*26*	*1793 (1843)*	*0.758*	*0.729 to 0.788*	Stratus	4	791 (765)	0.819	0.786 to 0.851
Spectralis	*11*	*806 (857)*	*0.759*	*0.704 to 0.814*	Temporal Outer				
RTVue	*12*	*1040 (895)*	*0.791*	*0.746 to 0.835*	Stratus	4	791 (765)	0.773	0.736 to 0.811
Topcon	*5*	*433 (294)*	*0.707*	*0.644 to 0.770*	Nasal Outer				
					Stratus	4	791 (765)	0.746	0.695 to 0.796
Macula—GCIPL					Superior Inner				
Average	20	1860 (1469)	0.864	0.837 to 0.890	Stratus	4	730 (708)	0.708	0.623 to 0.793
Cirrus	*14*	*1308 (1146)*	*0.880*	*0.851 to 0.910*	Inferior Inner				
Topcon	*5*	*475 (264)*	*0.805*	*0.767 to 0.843*	Stratus	4	791 (765)	0.755	0.695 to 0.816
Inferior	21	1804 (1547)	0.861	0.836 to 0.886	Temporal Inner				
Cirrus	*13*	*1245 (1095)*	*0.874*	*0.839 to 0.908*	Stratus	4	791 (765)	0.742	0.691 to 0.792
Spectralis	*2*	*120 (120)*	*0.841*	*0.791 to 0.890*	Nasal Inner				
Topcon	*6*	*439 (332)*	*0.841*	*0.809 to 0.872*	Stratus	4	730 (708)	0.670	0.549 to 0.790
Superior	21	1804 (1547)	0.787	0.751 to 0.823					
Cirrus	*13*	*1245 (1095)*	*0.825*	*0.786 to 0.864*					
Spectralis	*2*	*120 (120)*	*0.697*	*0.629 to 0.765*					
Topcon	*6*	*439 (332)*	*0.734*	*0.693 to 0.775*					
Nasal	4	240 (240)	0.647	0.589 to 0.704					
Spectralis	*2*	*120 (120)*	*0.668*	*0.599 to 0.737*					
Topcon	*2*	*120 (120)*	*0.624*	*0.534 to 0.715*					
Temporal	4	240 (240)	0.811	0.747 to 0.876					
Spectralis	*2*	*120 (120)*	*0.811*	*0.686 to 0.936*					
Topcon	*2*	*120 (120)*	*0.806*	*0.753 to 0.860*					
Superotemporal	13	1018 (927)	0.835	0.792 to 0.877					

(*Continued*)

Table 3. (*Continued*)

Perimetric Glaucoma–Pooled AUROCs (if I^2 > 50% random effects meta-analysis was used, if I^2 < 50% fixed effects was used)									
Test Parameter, Location and OCT Device	**Number of Studies**	**Pooled Sample Size**	**Pooled AUROC**	**95% CI**	**Test Parameter, Location and OCT Device**	**Number of Studies**	**Pooled Sample Size**	**Pooled AUROC**	**95% CI**
Cirrus	11	835 (827)	0.840	0.793 to 0.887					
Superonasal	13	1018 (927)	0.778	0.727 to 0.829					
Cirrus	11	835 (827)	0.789	0.734 to 0.844					
Inferotemporal	13	1018 (927)	0.879	0.848 to 0.910					
Cirrus	11	835 (827)	0.874	0.838 to 0.909					
Inferonasal	13	1018 (927)	0.789	0.752 to 0.827					
Cirrus	11	835 (827)	0.792	0.745 to 0.838					
Minimum									
Cirrus	10	777 (780)	0.904	0.875 to 0.933					

https://doi.org/10.1371/journal.pone.0190621.t003

0.935 to 0.972)–had similar AUROCs. Superior macular GCC (0.856, CI95% 0.837 to 0.876), performed worse than the remainder of the macular GCC parameters. RNFL and macular GCC have comparable AUROCs (average RNFL (0.959, CI95% 0.946 to 0.972), macula GCC (0.938, CI95% 0.911 to 0.965)).

Myopic patients. AUROCs of OCT for glaucoma diagnosis in myopic patients are summarized in Table 7, and illustrated in Fig 8. All OCT devices performed relatively similarly for glaucoma diagnosis. Within RNFL, the average (0.917, CI95% 0.884 to 0.950), inferior (0.937, CI95% 0.920 to 0.955), superior (0.880, CI95% 0.855 to 0.906), and temporal (0.854, CI95% 0.822 to 0.886) parameters had improved AUROC compared to the nasal area (0.617, CI95% 0.556 to 0.679). For both macular GCIPL and macular GCC scans, diagnostic performance of all individual parameters was similar. In addition, there were no notable differences in AUROC for the average parameters of RNFL (0.917, CI95% 0.884 to 0.950), macular GCIPL (0.905, CI95% 0.859 to 0.952), and macular GCC (0.953, CI95% 0.936 to 0.971) scans.

Evaluation of publication bias

Funnel plots were constructed to evaluate publication bias in the meta-analysis. Several funnel plots were created, one for each imaging parameter (average, superior, inferior etc.), of each area (RNFL, macula), for each OCT device, within each patient subgroup. No pattern was evident, ie. no one patient group, OCT device, or scan type/parameter was noted to be more likely to have publication bias.

Discussion

This meta-analysis demonstrates that OCT is a valuable adjunctive tool to aid in glaucoma diagnosis. Pooled estimates of diagnostic accuracy (AUROC) for the most commonly used OCT instruments (Zeiss Cirrus OCT, Zeiss, Stratus OCT, Heidelberg Spectralis, Optovue RTVue, Topcon 3D-OCT) were determined based upon their ability to differentiate between

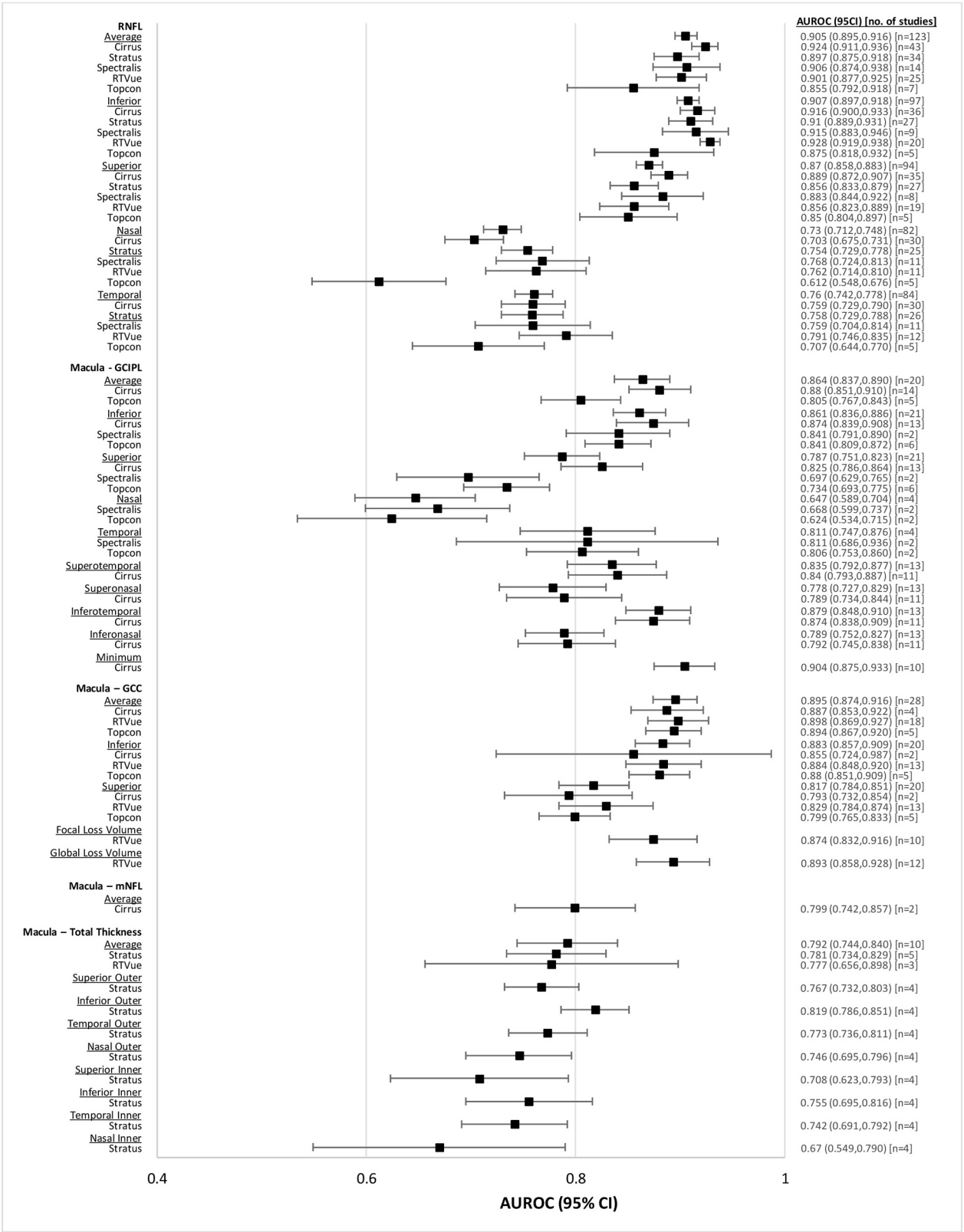

Fig 4. Forest plot of diagnostic accuracies of RNFL and macular OCT parameters, perimetric glaucoma.

https://doi.org/10.1371/journal.pone.0190621.g004

Table 4. Pooled AUROCs of RNFL and macular OCT parameters for pre-perimetric glaucoma patients.

Pre—Perimetric Glaucoma–Pooled AUROCs (if I^2 > 50% random effects meta-analysis was used, if I^2 < 50% fixed effects was used)									
Test Parameter, Location and OCT Device	**Number of Patient Groups**	**Pooled Sample Size (controls)**	**Pooled AUROC**	**95% CI**	**Test Parameter, Location and OCT Device**	**Number of Studies**	**Pooled Sample Size**	**Pooled AUROC**	**95% CI**
RNFL					**Macula—GCC**				
Average	36	1664 (2541)	0.831	0.808 to 0.854	Average	10	526 (525)	0.797	0.768 to 0.825
Cirrus	14	622 (1186)	0.835	0.800 to 0.871	RTVue	6	365 (333)	0.797	0.762 to 0.833
Stratus	10	399 (565)	0.834	0.780 to 0.887	Topcon	3	112 (141)	0.789	0.712 to 0.867
Spectralis	4	208 (341)	0.850	0.819 to 0.881	Inferior	8	425 (409)	0.803	0.773 to 0.833
RTVue	5	313 (268)	0.814	0.748 to 0.880	RTVue	5	313 (268)	0.81	0.774 to 0.847
Topcon	3	122 (181)	0.798	0.744 to 0.851	Topcon	3	112 (141)	0.788	0.719 to 0.857
Inferior	28	1256 (1748)	0.828	0.801 to 0.855	Superior	8	425 (409)	0.755	0.722 to 0.788
Cirrus	19	834 (1225)	0.827	0.793 to 0.860	RTVue	5	313 (268)	0.765	0.713 to 0.818
Stratus	7	299 (420)	0.815	0.763 to 0.867	Topcon	3	112 (141)	0.69	0.623 to 0.756
RTVue	5	313 (268)	0.818	0.767 to 0.868	Focal Loss Volume				
Topcon	3	122 (181)	0.812	0.759 to 0.865	RTVue	5	249 (281)	0.769	0.722 to 0.815
Superior	27	1256 (1711)	0.774	0.740 to 0.809	Global Loss Volume				
Cirrus	11	487 (770)	0.811	0.757 to 0.864	RTVue	5	249 (281)	0.824	0.787 to 0.862
Stratus	7	299 (420)	0.743	0.676 to 0.810					
RTVue	5	313 (268)	0.787	0.723 to 0.852	**Macula—GCIPL**				
Topcon	3	122 (181)	0.734	0.677 to 0.791	Average	9	395 (732)	0.762	0.708 to 0.816
Nasal	24	1025 (1560)	0.645	0.610 to 0.680	Cirrus	5	205 (487)	0.791	0.722 to 0.859
Cirrus	11	487 (770)	0.636	0.580 to 0.692	Topcon	4	190 (245)	0.716	0.664 to 0.767
Stratus	7	299 (420)	0.657	0.594 to 0.720	Inferior	8	346 (681)	0.756	0.690 to 0.823
Spectralis	3	131 (244)	0.666	0.607 to 0.724	Cirrus	4	156 (436)	0.780	0.685 to 0.875
Topcon	2	82 (106)	0.583	0.498 to 0.669	Topcon	4	190 (245)	0.728	0.651 to 0.806
Temporal	24	1025 (1570)	0.667	0.627 to 0.707	Superior	7	278 (617)	0.739	0.703 to 0.775
Cirrus	11	487 (770)	0.695	0.624 to 0.767	Cirrus	4	156 (436)	0.754	0.712 to 0.797
Stratus	7	299 (420)	0.630	0.591 to 0.669	Topcon	3	122 (181)	0.697	0.627 to 0.767
Spectralis	3	131 (244)	0.638	0.581 to 0.695					

(*Continued*)

Table 4. (*Continued*)

Pre—Perimetric Glaucoma–Pooled AUROCs (if I^2 > 50% random effects meta-analysis was used, if I^2 < 50% fixed effects was used)									
Test Parameter, Location and OCT Device	**Number of Patient Groups**	**Pooled Sample Size (controls)**	**Pooled AUROC**	**95% CI**	**Test Parameter, Location and OCT Device**	**Number of Studies**	**Pooled Sample Size**	**Pooled AUROC**	**95% CI**
Topcon	2	82 (106)	0.63	0.545 to 0.716					

https://doi.org/10.1371/journal.pone.0190621.t004

normal participants and glaucoma patients. A summary of the technical features of each device are outlined in Table 8.

The 150 studies included reported the diagnostic capability of several RNFL and macular parameters. Macular scans were further subdivided by retinal segmentation (GCC, GCIPL, mNFL or total retinal thickness). The AUROCs for average, superior and inferior RNFL parameters were larger than for nasal and temporal areas, a finding that was consistent for the overall patient group, as well as glaucoma subgroups. This finding is explained by the work of Traynis et al., 2014 who proposed a schematic of glaucomatous damage to the macula. Retinal ganglion cells (RCGs) in the regions of the macula most vulnerable to glaucomatous damage (inferior macula and region outside of the central 8 degrees of macula), project to the inferior and superior quadrants of the optic disc. Whereas RCGs in the less vulnerable regions (superior macula), project to the temporal region of the disc [179].

By comparison, in the macular GCIPL scans, we found that the inferonasal and superonasal parameters had poorer diagnostic efficacy than the average, superior, inferior, and temporal (infero- and superotemporal parameters). These differences between parameters were not found in the macular GCC scans.

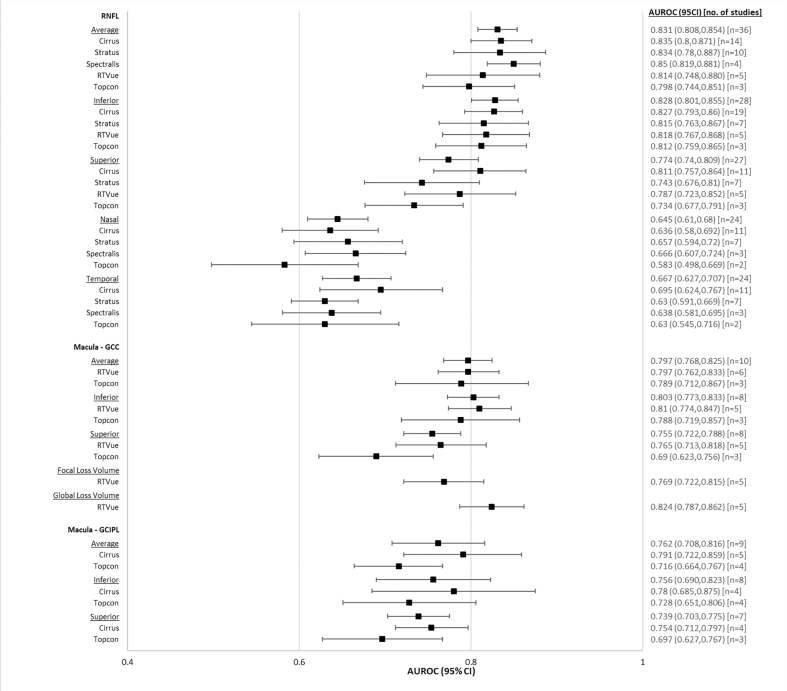

Fig 5. Forest plot of diagnostic accuracies of RNFL and macular OCT parameters, pre-perimetric glaucoma.

https://doi.org/10.1371/journal.pone.0190621.g005

Table 5. Pooled AUROCs of RNFL and macular OCT parameters for mild glaucoma patients.

Mild Glaucoma–Pooled AUROCs (if I^2 > 50% random effects meta-analysis was used, if I^2 < 50% fixed effects was used)									
Test Parameter, Location and OCT Device	**Number of Studies**	**Pooled Sample Size**	**Pooled AUROC**	**95% CI**	**Test Parameter, Location and OCT Device**	**Number of Studies**	**Pooled Sample Size**	**Pooled AUROC**	**95% CI**
RNFL					**Macula—GCC**				
Average	34	2146 (2782)	0.907	0.885 to 0.928	Average	13	817 (836)	0.861	0.819 to 0.903
Cirrus	12	990 (1409)	0.933	0.912 to 0.953	Cirrus	2	143 (128)	0.807	0.667 to 0.948
Stratus	5	225 (308)	0.909	0.838 to 0.980	RTVue	8	467 (540)	0.857	0.807 to 0.907
Spectralis	5	193 (282)	0.928	0.915 to 0.942	Topcon	3	207 (168)	0.901	0.820 to 0.982
RTVue	8	467 (540)	0.847	0.781 to 0.913					
Topcon	4	271 (243)	0.919	0.884 to 0.953	Inferior	10	686 (721)	0.850	0.807 to 0.894
					Cirrus	2	143 (128)	0.814	0.686 to 0.941
Inferior	26	1724 (2393)	0.897	0.874 to 0.919	RTVue	5	336 (425)	0.837	0.791 to 0.883
Cirrus	10	808 (1253)	0.921	0.896 to 0.946	Topcon	3	207 (168)	0.890	0.808 to 0.973
Stratus	3	171 (232)	0.899	0.839 to 0.959					
Spectralis	4	138 (240)	0.917	0.903 to 0.932	Superior	10	686 (721)	0.789	0.763 to 0.815
RTVue	5	336 (425)	0.826	0.763 to 0.890	Cirrus	2	143 (128)	0.761	0.680 to 0.841
Topcon	4	271 (243)	0.904	0.869 to 0.939	RTVue	5	336 (425)	0.776	0.722 to 0.831
					Topcon	3	207 (168)	0.814	0.771 to 0.857
Superior	26	1720 (2393)	0.854	0.827 to 0.882					
Cirrus	10	808 (1253)	0.886	0.855 to 0.917					
Stratus	3	167 (232)	0.833	0.712 to 0.954					
Spectralis	4	138 (240)	0.871	0.845 to 0.897					
RTVue	5	336 (425)	0.784	0.725 to 0.843					
Topcon	4	271 (243)	0.833	0.785 to 0.882					
Nasal	20	1302 (1549)	0.698	0.664 to 0.733					
Cirrus	9	700 (745)	0.667	0.619 to 0.716					
Stratus	3	171 (232)	0.706	0.622 to 0.791					
Spectralis	3	88 (190)	0.736	0.648 to 0.825					
RTVue	3	200 (254)	0.769	0.721 to 0.818					

(*Continued*)

Table 5. (*Continued*)

Mild Glaucoma–Pooled AUROCs (if I^2 > 50% random effects meta-analysis was used, if I^2 < 50% fixed effects was used)									
Test Parameter, Location and OCT Device	**Number of Studies**	**Pooled Sample Size**	**Pooled AUROC**	**95% CI**	**Test Parameter, Location and OCT Device**	**Number of Studies**	**Pooled Sample Size**	**Pooled AUROC**	**95% CI**
Topcon	2	143 (128)	0.644	0.560 to 0.728					
Temporal	20	1302 (1549)	0.726	0.690 to 0.762					
Cirrus	9	700 (745)	0.738	0.698 to 0.779					
Stratus	3	171 (232)	0.684	0.583 to 0.785					
Spectralis	3	88 (190)	0.771	0.688 to 0.854					
RTVue	3	200 (254)	0.702	0.570 to 0.833					
Topcon	2	143 (128)	0.730	0.649 to 0.810					

https://doi.org/10.1371/journal.pone.0190621.t005

Comparing between different scan types, RNFL thickness, macular GCIPL and macular GCC had similar diagnostic capability to differentiate between normal and glaucomatous eyes. Total macular thickness had lower AUROC for glaucoma diagnosis than these more specific scan types. Through stratification of patients by disease severity for sub-analysis, we also note that the diagnostic capability of OCT improves with increased disease severity.

One major question we wished to address through this review was whether there were instrument-dependent differences in diagnostic ability of OCT. It appears that for the majority of subgroups, there are no notable differences between devices.

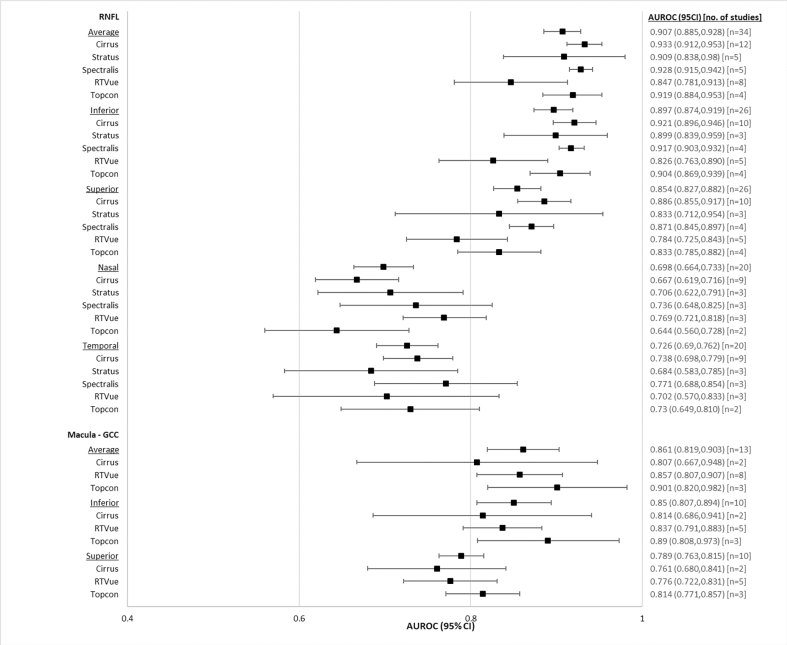

Fig 6. Forest plot of diagnostic accuracies of RNFL and macular OCT parameters, mild glaucoma.

https://doi.org/10.1371/journal.pone.0190621.g006

Table 6. Pooled AUROCs of RNFL and macular OCT parameters for moderate to severe glaucoma patients.

Moderate to Severe Glaucoma–Pooled AUROCs (if I^2 > 50% random effects meta-analysis was used, if I^2 < 50% fixed effects was used)									
Test Parameter, Location and OCT Device	**Number of Studies**	**Pooled Sample Size**	**Pooled AUROC**	**95% CI**	**Test Parameter, Location and OCT Device**	**Number of Studies**	**Pooled Sample Size**	**Pooled AUROC**	**95% CI**
RNFL					**Macula—GCC**				
Average	15	752 (1465)	0.964	0.951 to 0.976	Average				
Cirrus	5	353 (857)	0.963	0.948 to 0.978	RTVue	7	299 (434)	0.938	0.906 to 0.969
Stratus	2	74 (109)	0.990	0.975 to 1.000					
RTVue	7	299 (434)	0.955	0.928 to 0.981	Inferior				
					RTVue	3	163 (274)	0.911	0.878 to 0.943
Inferior	8	485 (1114)	0.953	0.934 to 0.972					
Cirrus	3	248 (701)	0.971	0.954 to 0.988	Superior				
RTVue	3	163 (274)	0.923	0.882 to 0.964	RTVue	3	163 (204)	0.852	0.832 to 0.872
Superior	8	485 (1114)	0.914	0.891 to 0.937	Focal Loss Volume				
Cirrus	3	248 (701)	0.930	0.901 to 0.958	RTVue	5	240 (364)	0.927	0.903 to 0.951
RTVue	3	163 (274)	0.884	0.848 to 0.920					
					Global Loss Volume				
					RTVue	5	240 (364)	0.926	0.903 to 0.949

https://doi.org/10.1371/journal.pone.0190621.t006

Comparison with other reviews

Previous reviews on the diagnostic capability of OCT for glaucoma have been published [14,181–185]. The present review has some unique advantages over previous reports. First, as mentioned previously, a wide gold standard was accepted for inclusion, ie. White-on-white

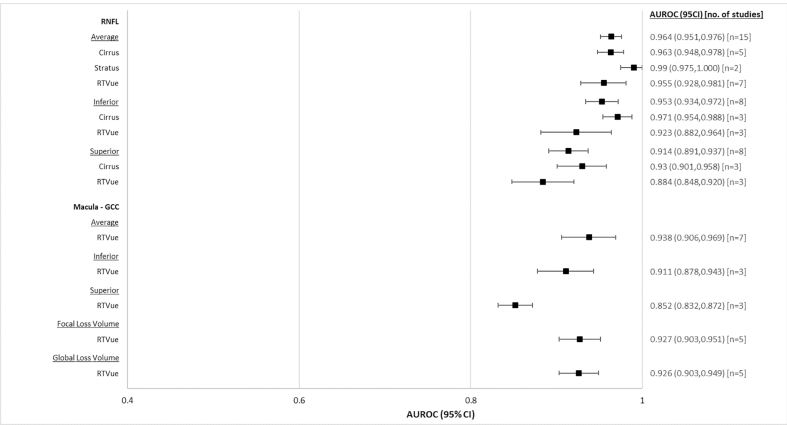

Fig 7. Forest plot of diagnostic accuracies of RNFL and macular OCT parameters, moderate to severe glaucoma.

https://doi.org/10.1371/journal.pone.0190621.g007

Table 7. Pooled AUROCs of RNFL and macular OCT parameters for myopic patients.

Myopic Patients–Pooled AUROCs (if I^2 > 50% random effects meta-analysis was used, if I^2 < 50% fixed effects was used)									
Test Parameter, Location and OCT Device	**Number of Studies**	**Pooled Sample Size**	**Pooled AUROC**	**95% CI**	**Test Parameter, Location and OCT Device**	**Number of Studies**	**Pooled Sample Size**	**Pooled AUROC**	**95% CI**
RNFL					**Macula—GCC**				
Average	11	586 (461)	0.917	0.884 to 0.950	Average	9	509 (411)	0.953	0.936 to 0.971
Cirrus	4	213 (157)	0.928	0.883 to 0.973	Cirrus	2	136 (107)	0.932	0.884 to 0.981
RTVue	5	237 (197)	0.875	0.807 to 0.942	RTVue	5	237 (197)	0.930	0.902 to 0.959
Topcon	2	136 (107)	0.951	0.921 to 0.982	Topcon	2	136 (107)	0.973	0.948 to 0.999
Inferior	10	534 (423)	0.937	0.920 to 0.955	Inferior	8	457 (373)	0.939	0.918 to 0.960
Cirrus	4	213 (157)	0.923	0.893 to 0.953	Cirrus	2	136 (107)	0.923	0.877 to 0.970
RTVue	4	185 (159)	0.913	0.867 to 0.959	RTVue	4	185 (159)	0.925	0.890 to 0.960
Topcon	2	136 (107)	0.959	0.930 to 0.988	Topcon	2	136 (107)	0.959	0.927 to 0.991
Superior	10	534 (423)	0.880	0.855 to 0.906	Superior	8	457 (313)	0.913	0.885 to 0.941
Cirrus	4	213 (157)	0.897	0.859 to 0.935	Cirrus	2	136 (107)	0.895	0.832 to 0.958
RTVue	4	185 (159)	0.839	0.775 to 0.902	RTVue	4	185 (159)	0.894	0.848 to 0.939
Topcon	2	136 (107)	0.876	0.819 to 0.932	Topcon	2	136 (107)	0.919	0.829 to 1.000
Nasal	8	485 (371)	0.617	0.556 to 0.679	Focal Loss Volume				
Cirrus	4	213 (157)	0.548	0.478 to 0.618	RTVue	3	101 (90)	0.898	0.828 to 0.969
RTVue	2	136 (107)	0.744	0.668 to 0.819					
Topcon	2	136 (107)	0.591	0.501 to 0.680	Global Loss Volume				
					RTVue	3	101 (90)	0.924	0.886 to 0.962
Temporal	8	485 (371)	0.854	0.822 to 0.886					
Cirrus	4	213 (157)	0.815	0.741 to 0.890					
RTVue	2	136 (107)	0.876	0.821 to 0.931					
Topcon	2	136 (107)	0.859	0.800 to 0.919					
Macula—GCIPL									
Average	6	349 (264)	0.905	0.859 to 0.952					
Cirrus	4	213 (157)	0.883	0.818 to 0.948					
Topcon	2	136 (107)	0.943	0.893 to 0.993					

(*Continued*)

Table 7. (*Continued*)

Myopic Patients–Pooled AUROCs (if I^2 > 50% random effects meta-analysis was used, if I^2 < 50% fixed effects was used)									
Test Parameter, Location and OCT Device	**Number of Studies**	**Pooled Sample Size**	**Pooled AUROC**	**95% CI**	**Test Parameter, Location and OCT Device**	**Number of Studies**	**Pooled Sample Size**	**Pooled AUROC**	**95% CI**
Inferior	6	349 (264)	0.918	0.887 to 0.950					
Cirrus	4	213 (157)	0.896	0.851 to 0.940					
Topcon	2	136 (107)	0.940	0.896 to 0.985					
Superior	6	349 (264)	0.851	0.789 to 0.914					
Cirrus	4	213 (157)	0.832	0.749 to 0.914					
Topcon	2	136 (107)	0.899	0.831 to 0.967					

https://doi.org/10.1371/journal.pone.0190621.t007

standard automated perimetry, optic disc appearance, elevated IOP, or any combination thereof. This wide gold standard more accurately reflects true clinical practice, where patients undergoing OCT to aid in glaucoma diagnosis may have undergone many of these other diagnostic modalities previously. The majority of previous reviews have limited inclusion criteria to those patients who have exclusively undergone standard automated perimetry. Our approach enabled the inclusion of 150 OCT studies, markedly larger than previous meta-analyses; a Cochrane review by Michelessi et al.[181] identified 63 OCT studies, Fallon et al.[185] identified 47 studies, Ahmed et al.[182] identified 84 studies, and Oddone et al.[183] identified 34 studies. The larger number of studies included enabled a more robust meta-analysis and the analyses of several patient subgroups.

Importantly, this meta-analysis provides pooled estimates of AUROCs, rather than sensitivity and specificity, as used in previous reviews. Only one other OCT review, by Chen et al.[184] identified reported pooled AUROCs; however, that review was limited to only 21 studies of Zeiss Stratus OCT. Reporting of AUROC is advantageous when describing the utility of a diagnostic test as it represents the diagnostic capability of the test regardless of specific cutoff used. We found that individual studies were inconstant in their reporting of sensitivity and specificity, with certain studies reporting sensitivities and particular specificity cutoffs, and others reporting the "optimal" sensitivity/specificity cutoff. Meta-analysis of such inconsistent data is difficult.

Limitations

One limitation of this study was the relatively large number of case-control studies that were captured in the inclusion criteria. The case-control design has been suggested to overestimate accuracy[186]. As the main purpose was to compare the diagnostic performance of the most common currently used OCT devices and none were found to be superior, this limitation unlikely introduced any significant bias. Another limitation may have resulted from choosing to the compare a number of macular parameters. Unlike RNFL scans, studies were quite heterogeneous in terms of which macular parameters were reported, ie. some reported GCIPL, GCC, mNFL, and total thickness. As such, these scan types had to be separated for meta-analysis, reducing sample sizes, and consequently increasing instability of AUROC estimates. Importantly, all studies included in the meta-analysis evaluated the ability to differentiate healthy controls from confirmed glaucoma patients, which does not reflect real clinical practice where many patients are undifferentiated.

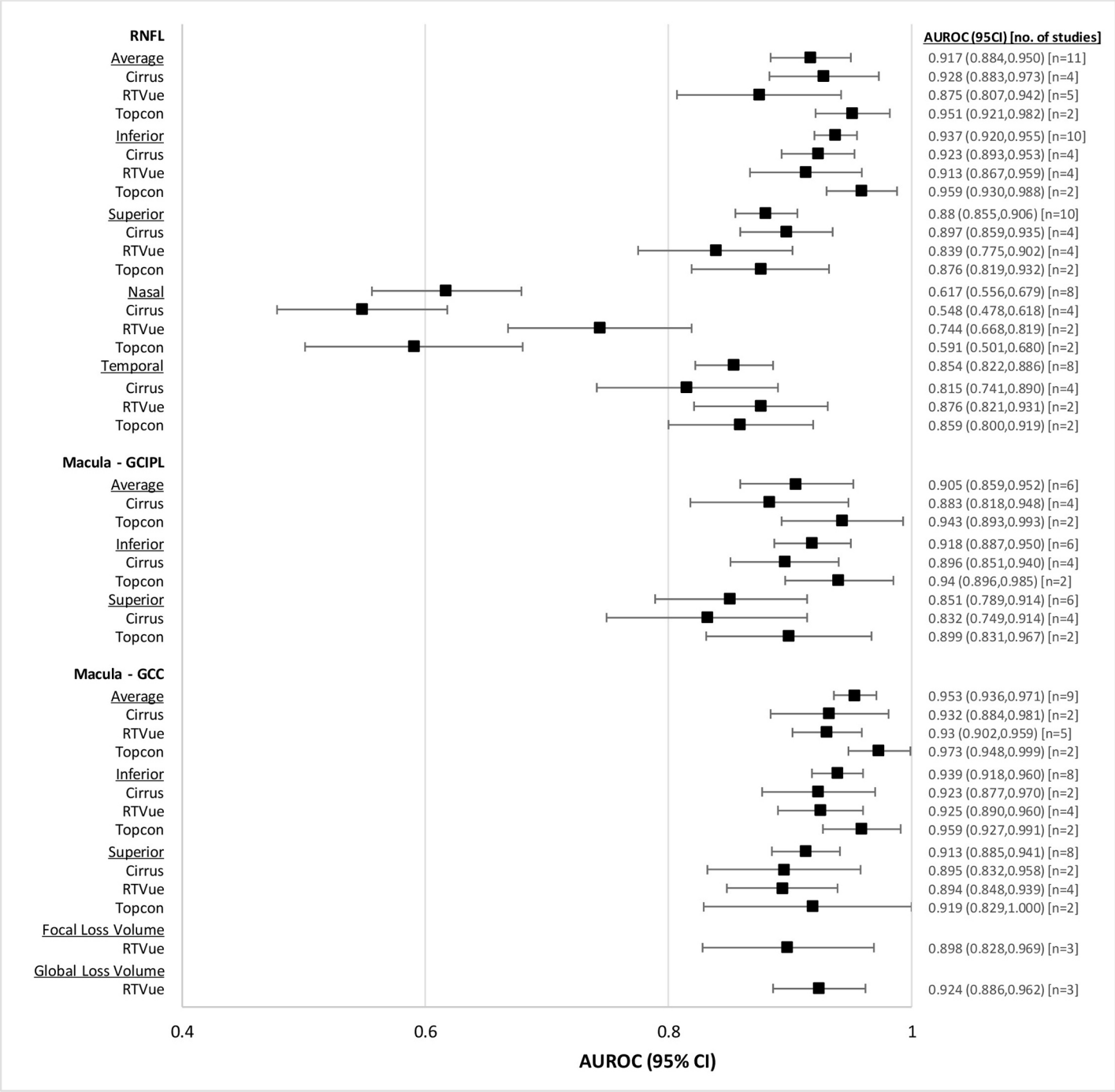

Fig 8. Forest plot of diagnostic accuracies of RNFL and macular OCT parameters, myopic patients.

https://doi.org/10.1371/journal.pone.0190621.g008

Conclusion

The currently available OCT devices (Zeiss Cirrus, Zeiss Stratus, Heidelberg Spectralis, Optovue RTVue, Topcon 3D-OCT) demonstrated good diagnostic accuracy in their ability to differentiate glaucoma patients from normal controls. This ability increased with the severity of the glaucoma. There was no major device-related differences in diagnostic capacity. Within

Table 8. Technical features of each of the OCT devices studied [27,180].

Model	Zeiss Stratus	Zeiss Cirrus	Heidelberg Spectralis	Optovue RTVue	Topcon 3D-OCT
Key Features	- Sequential acquisition	- Simultaneous acquisition			
	- 1 pixel at a time	- Entire A-scan collected at once			
	- Utilizes a mirror	- Faster than eye movements			
		- Does not utilize a mirror			
		- Analyzes data using a spectrometer			
Scanning Speed (A-scans/sec)	400	27,000–68,000	40,000	70,000	27,000
Axial resolution (microns)	10	5	3.9	5	5–6
Imaging modes available	TD-OCT	SD-OCT	SD-OCT	SD-OCT	SD-OCT
		cLSO	IR fundus photo with cLSO		
Scanning range	Retina/nerve	Retina/nerve	Retina/nerve	Retina/nerve	Retina/nerve
		Anterior segment		Cornea	Anterior segment
				Angle	
Posterior Segment Analyses	Macula: Total thickness	Macula: Macular thickness, macular changes, ganglion cells, RPE changes	Macula: Real-time, fast, dense, detail, posterior pole, seven lines	Macula: Retinal trend analysis, ganglion cell complex, retinal overview report, multilayers en face report	Macula: 3D macula report, macular drusen analysis
	Nerve: RNFL thickness	Nerve: RNFL thickness, guided progression	Nerve: Fast, dense, posterior pole, nerve head circle	Nerve: Retinal nerve fiber and optic disc, optic disc structure and analysis	Nerve: 3D disc report, RNFL trend analysis, glaucoma analysis
		3D imaging		Wide-field en face mapping	Glaucoma and macula report (12 × 9 mm)
				Combined RNFL and ganglion cell change report	

cLSO: confocal laser scanning ophthalmoscope; TD-OCT: time domain optical coherence tomography; SD-OCT: spectral domain optical coherence tomography; RNFL: retinal nerve fiber layer

https://doi.org/10.1371/journal.pone.0190621.t008

RNFL scans, the nasal and temporal parameters are more poorly diagnostic than the average, superior and inferior parameters. Across all macular GCIPL scans, the nasal (supero- and infero-nasal) parameters had lower AUROCs than the average, superior, inferior and temporal regions. The diagnostic capacity of RNFL is similar to segmented macular regions (GCIPL, GCC), and better than total macular thickness. As OCT technology continues to evolve at a faster pace than functional assessments of optic nerve health, future studies will be needed to fully understand its role in glaucoma management.

Supporting information

S1 Table. Appendix 1 –Search strategies.
(PDF)

S2 Table. Appendix 2 –Individual study characteristics.
(PDF)

S3 Table. PRISMA Checklist.
(DOC)

Author Contributions

Conceptualization: Vinay Kansal, James J. Armstrong, Cindy Hutnik.

Data curation: Vinay Kansal, James J. Armstrong, Robert Pintwala.

Formal analysis: Vinay Kansal, James J. Armstrong, Robert Pintwala.

Investigation: Vinay Kansal, James J. Armstrong.

Methodology: Vinay Kansal, James J. Armstrong, Cindy Hutnik.

Project administration: James J. Armstrong, Cindy Hutnik.

Supervision: Vinay Kansal, Cindy Hutnik.

Validation: Vinay Kansal.

Visualization: James J. Armstrong.

Writing – original draft: Vinay Kansal, James J. Armstrong.

Writing – review & editing: Vinay Kansal, James J. Armstrong, Robert Pintwala, Cindy Hutnik.

References

1. Pascolini D, Mariotti SP. Global estimates of visual impairment: 2010. Br J Ophthalmol. 2012; 96: 614–618. https://doi.org/10.1136/bjophthalmol-2011-300539 PMID: 22133988
2. Quigley HA. The number of people with glaucoma worldwide in 2010 and 2020. Br J Ophthalmol. 2006; 90: 262–267. https://doi.org/10.1136/bjo.2005.081224 PMID: 16488940
3. Quigley HA. Number of people with glaucoma worldwide. Br J Ophthalmol. 1996; 80: 389–393. https://doi.org/10.1136/bjo.80.5.389 PMID: 8695555
4. Tham Y-C, Li X, Wong TY, Quigley HA, Aung T, Cheng C-Y. Global Prevalence of Glaucoma and Projections of Glaucoma Burden through 2040: A Systematic Review and Meta-Analysis. Ophthalmology. 2014; 121: 2081–2090. https://doi.org/10.1016/j.ophtha.2014.05.013 PMID: 24974815
5. Quigley HA. Glaucoma. Lancet Lond Engl. 2011; 377: 1367–1377. https://doi.org/10.1016/S0140-6736(10)61423-7
6. Quigley HA, Katz J, Derick RJ, Gilbert D, Sommer A. An Evaluation of Optic Disc and Nerve Fiber Layer Examinations in Monitoring Progression of Early Glaucoma Damage. Ophthalmology. 1992; 99: 19–28. https://doi.org/10.1016/S0161-6420(92)32018-4 PMID: 1741133
7. Medeiros FA, Zangwill LM, Bowd C, Sample PA, Weinreb RN. Use of Progressive Glaucomatous Optic Disk Change as the Reference Standard for Evaluation of Diagnostic Tests in Glaucoma. Am J Ophthalmol. 2005; 139: 1010–1018. https://doi.org/10.1016/j.ajo.2005.01.003 PMID: 15953430
8. Greenfield DS, Weinreb RN. Role of Optic Nerve Imaging in Glaucoma Clinical Practice and Clinical Trials. Am J Ophthalmol. 2008; 145: 598–603.e1. https://doi.org/10.1016/j.ajo.2007.12.018 PMID: 18295183
9. Sharma P, Sample PA, Zangwill LM, Schuman JS. Diagnostic Tools for Glaucoma Detection and Management. Surv Ophthalmol. 2008; 53: S17–S32. https://doi.org/10.1016/j.survophthal.2008.08.003 PMID: 19038620
10. Bowd C, Weinreb RN, Williams JM, Zangwill LM. The Retinal Nerve Fiber Layer Thickness in Ocular Hypertensive, Normal, and Glaucomatous Eyes With Optical Coherence Tomography. Arch Ophthalmol. 2000; 118: 22–26. https://doi.org/10.1001/archopht.118.1.22 PMID: 10636409
11. Hrynchak P, Simpson T. Optical coherence tomography: an introduction to the technique and its use. Optom Vis Sci Off Publ Am Acad Optom. 2000; 77: 347–356.
12. Kee C, Cho C. Evaluation of retinal nerve fiber layer thickness in the area of apparently normal hemifield in glaucomatous eyes with optical coherence tomography. J Glaucoma. 2003; 12: 250–254. PMID: 12782844

13. Schuman JS, Hee MRM, Arya AV, Pedut-Kloizman T, Puliafito CA, Fujimoto JG, et al. Optical coherence tomography: A new tool for glaucoma diagnosis. Curr Opin Ophthalmol. 1995; 6: 89–95. PMID: 10150863

14. Bussel II, Wollstein G, Schuman JS. OCT for glaucoma diagnosis, screening and detection of glaucoma progression. Br J Ophthalmol. 2014; 98: ii15–ii19. https://doi.org/10.1136/bjophthalmol-2013-304326 PMID: 24357497

15. Sung KR, Kim JS, Wollstein G, Folio L, Kook MS, Schuman JS. Imaging of the retinal nerve fibre layer with spectral domain optical coherence tomography for glaucoma diagnosis. Br J Ophthalmol. 2011; 95: 909–914. https://doi.org/10.1136/bjo.2010.186924 PMID: 21030413

16. Leung CK, Cheung CYL, Weinreb RN, Qiu K, Liu S, Li H, et al. Evaluation of Retinal Nerve Fiber Layer Progression in Glaucoma: A Study on Optical Coherence Tomography Guided Progression Analysis. Invest Ophthalmol Vis Sci. 2010; 51: 217–222. https://doi.org/10.1167/iovs.09-3468 PMID: 19684001

17. Reus NJ, Lemij HG, Garway-Heath DF, Airaksinen PJ, Anton A, Bron AM, et al. Clinical Assessment of Stereoscopic Optic Disc Photographs for Glaucoma: The European Optic Disc Assessment Trial. Ophthalmology. 2010; 117: 717–723. https://doi.org/10.1016/j.ophtha.2009.09.026 PMID: 20045571

18. Oddone F, Centofanti M, Tanga L, Parravano M, Michelessi M, Schiavone M, et al. Influence of Disc Size on Optic Nerve Head versus Retinal Nerve Fiber Layer Assessment for Diagnosing Glaucoma. Ophthalmology. 2011; 118: 1340–1347. https://doi.org/10.1016/j.ophtha.2010.12.017 PMID: 21474186

19. Zeimer R, Asrani S, Zou S, Quigley H, Jampel H. Quantitative detection of glaucomatous damage at the posterior pole by retinal thickness mapping. Ophthalmology. 1998; 105: 224–231. https://doi.org/10.1016/S0161-6420(98)92743-9 PMID: 9479279

20. Guedes V, Schuman JS, Hertzmark E, Wollstein G, Correnti A, Mancini R, et al. Optical coherence tomography measurement of macular and nerve fiber layer thickness in normal and glaucomatous human eyes. Ophthalmology. 2003; 110: 177–189. PMID: 12511364

21. Medeiros FA, Zangwill LM, Bowd C, Vessani RM, Susanna R, Weinreb RN. Evaluation of retinal nerve fiber layer, optic nerve head, and macular thickness measurements for glaucoma detection using optical coherence tomography. Am J Ophthalmol. 2005; 139: 44–55. https://doi.org/10.1016/j.ajo.2004.08.069 PMID: 15652827

22. Leung CKS, Chan W-M, Yung W-H, Ng ACK, Woo J, Tsang M-K, et al. Comparison of macular and peripapillary measurements for the detection of glaucoma. Ophthalmology. 2005; 112: 391–400. https://doi.org/10.1016/j.ophtha.2004.10.020 PMID: 15745764

23. Mori S, Hangai M, Sakamoto A, Yoshimura N. Spectral-domain Optical Coherence Tomography Measurement of Macular Volume for Diagnosing Glaucoma: J Glaucoma. 2010; 19: 528–534. https://doi.org/10.1097/IJG.0b013e3181ca7acf PMID: 20164794

24. Tan O, Chopra V, Lu AT-H, Schuman JS, Ishikawa H, Wollstein G, et al. Detection of Macular Ganglion Cell Loss in Glaucoma by Fourier-Domain Optical Coherence Tomography. Ophthalmology. 2009; 116: 2305–2314.e2. https://doi.org/10.1016/j.ophtha.2009.05.025 PMID: 19744726

25. Nakatani Y, Higashide T, Ohkubo S, Takeda H, Sugiyama K. Evaluation of macular thickness and peripapillary retinal nerve fiber layer thickness for detection of early glaucoma using spectral domain optical coherence tomography. J Glaucoma. 2011; 20: 252–259. https://doi.org/10.1097/IJG.0b013e3181e079ed PMID: 20520570

26. Girkin CA, Liebmann J, Fingeret M, Greenfield DS, Medeiros F. The effects of race, optic disc area, age, and disease severity on the diagnostic performance of spectral-domain optical coherence tomography. Invest Ophthalmol Vis Sci. 2011; 52: 6148–6153. https://doi.org/10.1167/iovs.10-6698 PMID: 21421879

27. Reichel E, Ho J, Duker JS. OCT Units: Which One Is Right for Me? Rev Ophthalmol. 2009;

28. Kotowski J, Wollstein G, Ishikawa H, Schuman JS. Imaging of the optic nerve and retinal nerve fiber layer: An essential part of glaucoma diagnosis and monitoring. Surv Ophthalmol. 2014; 59: 458–467. https://doi.org/10.1016/j.survophthal.2013.04.007 PMID: 24388709

29. Moher D, Liberati A, Tetzlaff J, Altman DG. Preferred reporting items for systematic reviews and meta-analyses: the PRISMA statement. Ann Intern Med. 2009; 151: 264–269. PMID: 19622511

30. Whiting PF, Rutjes AWS, Westwood ME, Mallett S, Deeks JJ, Reitsma JB, et al. QUADAS-2: a revised tool for the quality assessment of diagnostic accuracy studies. Ann Intern Med. 2011; 155: 529–536. https://doi.org/10.7326/0003-4819-155-8-201110180-00009 PMID: 22007046

31. Zhou X-H, McClish DK, Obuchowski NA. Statistical methods in diagnostic medicine. New York: John Wiley & Sons, Ltd; 2009.

32. Hodapp E, Parrish RI, Anderson D. Clinical decisions in glaucoma. St. Louis: The CV Mosby Co; 1993.

33. Ajtony C, Balla Z, Somoskeoy S, Kovacs B. Relationship between Visual Field Sensitivity and Retinal Nerve Fiber Layer Thickness as Measured by Optical Coherence Tomography. Investig Opthalmology Vis Sci. 2007; 48: 258. https://doi.org/10.1167/iovs.06-0410 PMID: 17197541

34. Akashi A, Kanamori A, Nakamura M, Fujihara M, Yamada Y, Negi A. The Ability of Macular Parameters and Circumpapillary Retinal Nerve Fiber Layer by Three SD-OCT Instruments to Diagnose Highly Myopic GlaucomaAbility of Macular Parameters. Invest Ophthalmol Vis Sci. 2013; 54: 6025–6032. https://doi.org/10.1167/iovs.13-12630 PMID: 23908182

35. Akashi A, Kanamori A, Nakamura M, Fujihara M, Yamada Y, Negi A. Comparative Assessment for the Ability of Cirrus, RTVue, and 3D-OCT to Diagnose Glaucoma. Investig Opthalmology Vis Sci. 2013; 54: 4478. https://doi.org/10.1167/iovs.12-11268 PMID: 23737470

36. Akashi A, Kanamori A, Ueda K, Inoue Y, Yamada Y, Nakamura M. The Ability of SD-OCT to Differentiate Early Glaucoma With High Myopia From Highly Myopic Controls and Nonhighly Myopic Controls. Investig Opthalmology Vis Sci. 2015; 56: 6573. https://doi.org/10.1167/iovs.15-17635 PMID: 26567476

37. Aptel F, Sayous R, Fortoul V, Beccat S, Denis P. Structure–Function Relationships Using Spectral-Domain Optical Coherence Tomography: Comparison With Scanning Laser Polarimetry. Am J Ophthalmol. 2010; 150: 825–833.e1. https://doi.org/10.1016/j.ajo.2010.06.011 PMID: 20851372

38. Arifoglu HB, Simavli H, Midillioglu I, Berk Ergun S, Simsek S. Comparison of Ganglion Cell and Retinal Nerve Fiber Layer Thickness in Pigment Dispersion Syndrome, Pigmentary Glaucoma, and Healthy Subjects with Spectral-domain OCT. Semin Ophthalmol. 2017; 32: 204–209. https://doi.org/10.3109/08820538.2015.1053623 PMID: 26291741

39. Arintawati P, Sone T, Akita T, Tanaka J, Kiuchi Y. The Applicability of Ganglion Cell Complex Parameters Determined From SD-OCT Images to Detect Glaucomatous Eyes: J Glaucoma. 2013; 22: 713–718. https://doi.org/10.1097/IJG.0b013e318259b2e1 PMID: 22668975

40. Asaoka R, Hirasawa K, Iwase A, Fujino Y, Murata H, Shoji N, et al. Validating the Usefulness of the "Random Forests" Classifier to Diagnose Early Glaucoma With Optical Coherence Tomography. Am J Ophthalmol. 2017; 174: 95–103. https://doi.org/10.1016/j.ajo.2016.11.001 PMID: 27836484

41. Badalà F, Nouri-Mahdavi K, Raoof DA, Leeprechanon N, Law SK, Caprioli J. Optic Disk and Nerve Fiber Layer Imaging to Detect Glaucoma. Am J Ophthalmol. 2007; 144: 724–732. https://doi.org/10.1016/j.ajo.2007.07.010 PMID: 17868631

42. Baskaran M, Ong E-L, Li J-L, Cheung CY, Chen D, Perera SA, et al. Classification Algorithms Enhance the Discrimination of Glaucoma from Normal Eyes Using High-Definition Optical Coherence TomographyClassification Algorithms and Glaucoma Diagnosis. Invest Ophthalmol Vis Sci. 2012; 53: 2314–2320. https://doi.org/10.1167/iovs.11-8035 PMID: 22427583

43. Begum VU, Addepalli UK, Yadav RK, Shankar K, Senthil S, Garudadri CS, et al. Ganglion Cell-Inner Plexiform Layer Thickness of High Definition Optical Coherence Tomography in Perimetric and Preperimetric GlaucomaDiagnostic Ability of GCIPL Parameters in Glaucoma. Invest Ophthalmol Vis Sci. 2014; 55: 4768–4775. https://doi.org/10.1167/iovs.14-14598 PMID: 25015361

44. Bertuzzi F, Benatti E, Esempio G, Rulli E, Miglior S. Evaluation of Retinal Nerve Fiber Layer Thickness Measurements for Glaucoma Detection: GDx ECC Versus Spectral-domain OCT. J Glaucoma. 2014; 23: 232–239. https://doi.org/10.1097/IJG.0b013e3182741afc PMID: 23970337

45. Bizios D, Heijl A, Bengtsson B. Integration and fusion of standard automated perimetry and optical coherence tomography data for improved automated glaucoma diagnostics. BMC Ophthalmol. 2011; 11: 20. https://doi.org/10.1186/1471-2415-11-20 PMID: 21816080

46. Blumberg DM, Dale E, Pensec N, Cioffi GA, Radcliffe N, Pham M, et al. Discrimination of Glaucoma Patients From Healthy Individuals Using Combined Parameters From Spectral-domain Optical Coherence Tomography in an African American Population: J Glaucoma. 2016; 25: e196–e203. https://doi.org/10.1097/IJG.0000000000000289 PMID: 26066503

47. Blumberg DM, De Moraes CG, Liebmann JM, Garg R, Chen C, Theventhiran A, et al. Technology and the Glaucoma Suspect. Investig Opthalmology Vis Sci. 2016; 57: OCT80. https://doi.org/10.1167/iovs.15-18931 PMID: 27409509

48. Bourne RR, Medeiros FA, Bowd C, Jahanbakhsh K, Zangwill LM, Weinreb RN. Comparability of retinal nerve fiber layer thickness measurements of optical coherence tomography instruments. Invest Ophthalmol Vis Sci. 2005; 46: 1280–1285. https://doi.org/10.1167/iovs.04-1000 PMID: 15790891

49. Brusini P, Salvetat ML, Zeppieri M, Tosoni C, Parisi L, Felletti M. Comparison between GDx VCC scanning laser polarimetry and Stratus OCT optical coherence tomography in the diagnosis of chronic glaucoma. Acta Ophthalmol Scand. 2006; 84: 650–655. https://doi.org/10.1111/j.1600-0420.2006.00747.x PMID: 16965496

50. Burgansky-Eliash Z, Wollstein G, Chu T, Ramsey JD, Glymour C, Noecker RJ, et al. Optical Coherence Tomography Machine Learning Classifiers for Glaucoma Detection: A Preliminary Study. Investig Opthalmology Vis Sci. 2005; 46: 4147. https://doi.org/10.1167/iovs.05-0366 PMID: 16249492

51. Calvo P, Ferreras A, Abadia B, Ara M, Figus M, Pablo LE, et al. Assessment of the Optic Disc Morphology Using Spectral-Domain Optical Coherence Tomography and Scanning Laser Ophthalmoscopy. BioMed Res Int. 2014; 2014: 1–6. https://doi.org/10.1155/2014/275654 PMID: 25110668

52. Cho JW, Sung KR, Hong JT, Um TW, Kang SY, Kook MS. Detection of Glaucoma by Spectral Domain-scanning Laser Ophthalmoscopy/Optical Coherence Tomography (SD-SLO/OCT) and Time Domain Optical Coherence Tomography: J Glaucoma. 2011; 20: 15–20. https://doi.org/10.1097/IJG.0b013e3181d1d332 PMID: 20436370

53. Choi YJ, Jeoung JW, Park KH, Kim DM. Glaucoma Detection Ability of Ganglion Cell-Inner Plexiform Layer Thickness by Spectral-Domain Optical Coherence Tomography in High Myopia. Investig Opthalmology Vis Sci. 2013; 54: 2296. https://doi.org/10.1167/iovs.12-10530 PMID: 23462754

54. Choi YJ, Jeoung JW, Park KH, Kim DM. Clinical Use of an Optical Coherence Tomography Linear Discriminant Function for Differentiating Glaucoma From Normal Eyes: J Glaucoma. 2016; 25: e162–e169. https://doi.org/10.1097/IJG.0000000000000210 PMID: 25580887

55. Dave P, Shah J. Diagnostic accuracy of posterior pole asymmetry analysis parameters of spectralis optical coherence tomography in detecting early unilateral glaucoma. Indian J Ophthalmol. 2015; 63: 837. https://doi.org/10.4103/0301-4738.171965 PMID: 26669335

56. DeLeo´n-Ortega JE, Arthur SN, McGwin G, Xie A, Monheit BE, Girkin CA. Discrimination between Glaucomatous and Nonglaucomatous Eyes Using Quantitative Imaging Devices and Subjective Optic Nerve Head Assessment. Investig Opthalmology Vis Sci. 2006; 47: 3374. https://doi.org/10.1167/iovs.05-1239 PMID: 16877405

57. Fang Y, Pan Y, Li M, Qiao R, Cai Y. Diagnostic capability of Fourier-Domain optical coherence tomography in early primary open angle glaucoma. Chin Med J (Engl). 2010; 123: 2045–2050.

58. Garudadri CS, Rao HL, Parikh RS, Jonnadula GB, Selvaraj P, Nutheti R, et al. Effect of Optic Disc Size and Disease Severity on the Diagnostic Capability of Glaucoma Imaging Technologies in an Indian Population: J Glaucoma. 2012; 21: 475–480. https://doi.org/10.1097/IJG.0b013e31821829f1 PMID: 21522023

59. Gunvant P, Zheng Y, Essock EA, Parikh RS, Prabakaran S, Babu JG, et al. Comparison of Shape-based Analysis of Retinal Nerve Fiber Layer Data Obtained From OCT and GDx-VCC: J Glaucoma. 2009; 18: 464–471. https://doi.org/10.1097/IJG.0b013e31818c6f2b PMID: 19680055

60. Gunvant P, Zheng Y, Essock EA, Parikh RS, Prabakaran S, Babu JG, et al. Application of shape-based analysis methods to OCT retinal nerve fiber layer data in glaucoma. J Glaucoma. 2007; 16: 543–548. https://doi.org/10.1097/IJG.0b013e318050ab65 PMID: 17873716

61. Gyatsho J, Kaushik S, Gupta A, Pandav SS, Ram J. Retinal nerve fiber layer thickness in normal, ocular hypertensive, and glaucomatous Indian eyes: an optical coherence tomography study. J Glaucoma. 2008; 17: 122–127. https://doi.org/10.1097/IJG.0b013e31814b9817 PMID: 18344758

62. Hirasawa H, Mayama C, Tomidokoro A, Araie M, Iwase A, Sugiyama K, et al. Diagnostic performance and reproducibility of circumpapillary retinal nerve fiber layer thickness measurement in 10-degree sectors in early stage glaucoma. Jpn J Ophthalmol. 2015; 59: 86–93. https://doi.org/10.1007/s10384-014-0366-9 PMID: 25523886

63. Hirashima T, Hangai M, Nukada M, Nakano N, Morooka S, Akagi T, et al. Frequency-doubling technology and retinal measurements with spectral-domain optical coherence tomography in preperimetric glaucoma. Graefes Arch Clin Exp Ophthalmol. 2013; 251: 129–137. https://doi.org/10.1007/s00417-012-2076-7 PMID: 22684903

64. Hoesl LM, Tornow RP, Schrems WA, Horn FK, Mardin CY, Kruse FE, et al. Glaucoma Diagnostic Performance of GDxVCC and Spectralis OCT on Eyes With Atypical Retardation Pattern: J Glaucoma. 2013; 22: 317–324. https://doi.org/10.1097/IJG.0b013e318237c8c5 PMID: 22027931

65. Holló G, Naghizadeh F, Vargha P. Accuracy of Macular Ganglion-Cell Complex Thickness to Total Retina Thickness Ratio to Detect Glaucoma in White Europeans: J Glaucoma. 2014; 23: e132–e137. https://doi.org/10.1097/IJG.0000000000000030 PMID: 24247997

66. Hong S, Seong GJ, Kim SS, Kang SY, Kim CY. Comparison of Peripapillary Retinal Nerve Fiber Layer Thickness Measured by Spectral vs. Time Domain Optical Coherence Tomography. Curr Eye Res. 2011; 36: 125–134. https://doi.org/10.3109/02713683.2010.533807 PMID: 21158587

67. Horn FK, Mardin CY, Bendschneider D, Jünemann AG, Adler W, Tornow RP. Frequency doubling technique perimetry and spectral domain optical coherence tomography in patients with early glaucoma. Eye. 2011; 25: 17–29. https://doi.org/10.1038/eye.2010.155 PMID: 21102494

68. Huang J-Y, Pekmezci M, Mesiwala N, Kao A, Lin S. Diagnostic Power of Optic Disc Morphology, Peripapillary Retinal Nerve Fiber Layer Thickness, and Macular Inner Retinal Layer Thickness in

Glaucoma Diagnosis With Fourier-domain Optical Coherence Tomography: J Glaucoma. 2011; 20: 87–94. https://doi.org/10.1097/IJG.0b013e3181d787b6 PMID: 20577117

69. Huang L, Fan N, Shen X, He J. Comparison of the diagnostic ability of retinal nerve fiber layer thickness measured using time domain and spectral domain optical coherence tomography in primary open angle glaucoma. Eye Sci. 2011; 26: 132–137, 142. https://doi.org/10.3969/j.issn.1000-4432.2011.03.002 PMID: 21913343

70. Hung K-C, Wu P-C, Chang H-W, Lai I-C, Tsai J-C, Lin P-W, et al. Macular parameters of Stratus optical coherence tomography for assessing glaucoma in high myopia: Macular parameters for glaucoma in high myopia. Clin Exp Optom. 2015; 98: 39–44. https://doi.org/10.1111/cxo.12227 PMID: 25349103

71. Hung K-C, Wu P-C, Poon Y-C, Chang H-W, Lai C, Tsai J-C, et al. Macular diagnostic ability in OCT for assessing glaucoma in high myopia. Optom Vis Sci. 2016; 93: 126–135. https://doi.org/10.1097/OPX.0000000000000776 PMID: 26704143

72. Hwang YH, Ahn SI, Ko SJ. Diagnostic ability of macular ganglion cell asymmetry for glaucoma: Ganglion cell asymmetry in glaucoma. Clin Experiment Ophthalmol. 2015; 43: 720–726. https://doi.org/10.1111/ceo.12545 PMID: 25939316

73. Hwang YH, Kim YY. Glaucoma Diagnostic Ability of Quadrant and Clock-Hour Neuroretinal Rim Assessment Using Cirrus HD Optical Coherence Tomography. Investig Opthalmology Vis Sci. 2012; 53: 2226. https://doi.org/10.1167/iovs.11-8689 PMID: 22410556

74. Jeoung JW, Choi YJ, Park KH, Kim DM. Macular Ganglion Cell Imaging Study: Glaucoma Diagnostic Accuracy of Spectral-Domain Optical Coherence Tomography. Investig Opthalmology Vis Sci. 2013; 54: 4422. https://doi.org/10.1167/iovs.12-11273 PMID: 23722389

75. Jeoung JW, Kim T-W, Weinreb RN, Kim SH, Park KH, Kim DM. Diagnostic Ability of Spectral-domain Versus Time-domain Optical Coherence Tomography in Preperimetric Glaucoma: J Glaucoma. 2014; 23: 299–306. https://doi.org/10.1097/IJG.0b013e3182741cc4 PMID: 23377582

76. Jeoung JW, Park KH. Comparison of Cirrus OCT and Stratus OCT on the ability to detect localized retinal nerve fiber layer defects in preperimetric glaucoma. Invest Ophthalmol Vis Sci. 2010; 51: 938–945. https://doi.org/10.1167/iovs.08-3335 PMID: 19797208

77. Jung H-H, Sung M-S, Heo H, Park S-W. Macular inner plexiform and retinal nerve fiber layer thickness in glaucoma. Optom Vis Sci. 2014; 91: 1320–1327. https://doi.org/10.1097/OPX.0000000000000392 PMID: 25237762

78. Kanamori A, Naka M, Akashi A, Fujihara M, Yamada Y, Nakamura M. Cluster Analyses of Grid-Pattern Display in Macular Parameters Using Optical Coherence Tomography for Glaucoma DiagnosisOptical Coherence Tomography in Glaucoma Diagnosis. Invest Ophthalmol Vis Sci. 2013; 54: 6401–6408. https://doi.org/10.1167/iovs.13-12805 PMID: 23989192

79. Kang SY, Sung KR, Na JH, Choi EH, Cho JW, Cheon MH, et al. Comparison Between Deviation Map Algorithm and Peripapillary Retinal Nerve Fiber Layer Measurements Using Cirrus HD-OCT in the Detection of Localized Glaucomatous Visual Field Defects: J Glaucoma. 2012; 21: 372–378. https://doi.org/10.1097/IJG.0b013e3182127ab1 PMID: 21430549

80. Kaushik S, Singh Pandav S, Ichhpujani P, Gupta A, Gupta P. Retinal nerve fiber layer measurement and diagnostic capability of spectral-domain versus time-domain optical coherence tomography. Eur J Ophthalmol. 2011; 21: 566–572. https://doi.org/10.5301/EJO.2011.6289 PMID: 21279977

81. Kiddee W, Tantisarasart T, Wangsupadilok B. Performance of optical coherence tomography for distinguishing between normal eyes, glaucoma suspect and glaucomatous eyes. J Med Assoc Thai. 2013; 96: 689–95. PMID: 23951826

82. Kim HJ, Lee S-Y, Park KH, Kim DM, Jeoung JW. Glaucoma Diagnostic Ability of Layer-by-Layer Segmented Ganglion Cell Complex by Spectral-Domain Optical Coherence Tomography. Investig Opthalmology Vis Sci. 2016; 57: 4799. https://doi.org/10.1167/iovs.16-19214 PMID: 27654408

83. Kim KE, Ahn SJ, Kim DM. Comparison of two different spectral domain optical coherence tomography devices in the detection of localized retinal nerve fiber layer defects. Jpn J Ophthalmol. 2013; 57: 347–358. https://doi.org/10.1007/s10384-013-0239-7 PMID: 23539100

84. Kim KE, Kim SH, Jeoung JW, Park KH, Kim TW, Kim DM. Comparison of ability of time-domain and spectral-domain optical coherence tomography to detect diffuse retinal nerve fiber layer atrophy. Jpn J Ophthalmol. 2013; 57: 529–539. https://doi.org/10.1007/s10384-013-0270-8 PMID: 24000036

85. Kim NR, Hong S, Kim JH, Rho SS, Seong GJ, Kim CY. Comparison of Macular Ganglion Cell Complex Thickness by Fourier-Domain OCT in Normal Tension Glaucoma and Primary Open-Angle Glaucoma: J Glaucoma. 2013; 22: 133–139. https://doi.org/10.1097/IJG.0b013e3182254cde PMID: 21701394

86. Kim NR, Kim JH, Kim CY, Jun I, Je Seong G, Lee ES. Comparison of the Optic Nerve Imaging by Time-Domain Optical Coherence Tomography and Fourier-Domain Optical Coherence Tomography in Distinguishing Normal Eyes From Those With Glaucoma: J Glaucoma. 2013; 22: 36–43. https://doi.org/10.1097/IJG.0b013e31821e85f3 PMID: 21623218

87. Kim NR, Lee ES, Seong GJ, Choi EH, Hong S, Kim CY. Spectral-domain optical coherence tomography for detection of localized retinal nerve fiber layer defects in patients with open-angle glaucoma. Arch Ophthalmol. 2010; 128: 1121–1128. https://doi.org/10.1001/archophthalmol.2010.204 PMID: 20837794

88. Kim NR, Lee ES, Seong GJ, Kim JH, An HG, Kim CY. Structure–function relationship and diagnostic value of macular ganglion cell complex measurement using Fourier-domain OCT in glaucoma. Invest Ophthalmol Vis Sci. 2010; 51: 4646–4651. https://doi.org/10.1167/iovs.09-5053 PMID: 20435603

89. Kim NR, Lee ES, Seong GJ, Kang SY, Kim JH, Hong S, et al. Comparing the ganglion cell complex and retinal nerve fibre layer measurements by Fourier domain OCT to detect glaucoma in high myopia. Br J Ophthalmol. 2011; 95: 1115–1121. https://doi.org/10.1136/bjo.2010.182493 PMID: 20805125

90. Kim YK, Yoo BW, Jeoung JW, Kim HC, Kim HJ, Park KH. Glaucoma-Diagnostic Ability of Ganglion Cell-Inner Plexiform Layer Thickness Difference Across Temporal Raphe in Highly Myopic Eyes. Investig Opthalmology Vis Sci. 2016; 57: 5856. https://doi.org/10.1167/iovs.16-20116 PMID: 27802515

91. Kim YJ, Kang MH, Cho HY, Lim HW, Seong M. Comparative study of macular ganglion cell complex thickness measured by spectral-domain optical coherence tomography in healthy eyes, eyes with preperimetric glaucoma, and eyes with early glaucoma. Jpn J Ophthalmol. 2014; 58: 244–251. https://doi.org/10.1007/s10384-014-0315-7 PMID: 24610541

92. Kita Y, Kita R, Takeyama A, Anraku A, Tomita G, Goldberg I. Relationship between macular ganglion cell complex thickness and macular outer retinal thickness: a spectral-domain optical coherence tomography study: Outer retinal thickness in glaucoma. Clin Experiment Ophthalmol. 2013; n/a-n/a. https://doi.org/10.1111/ceo.12089 PMID: 23433351

93. Kita Y, Kita R, Takeyama A, Takagi S, Nishimura C, Tomita G. Ability of Optical Coherence Tomography–determined Ganglion Cell Complex Thickness to Total Retinal Thickness Ratio to Diagnose Glaucoma: J Glaucoma. 2013; 22: 757–762. https://doi.org/10.1097/IJG.0b013e31825af58a PMID: 22668980

94. Koh KM, Jin S, Hwang YH. Cirrus High-definition Optical Coherence Tomography Versus Spectral Optical Coherence Tomography/Scanning Laser Ophthalmoscopy in the Diagnosis of Glaucoma. Curr Eye Res. 2014; 39: 62–68. https://doi.org/10.3109/02713683.2013.824989 PMID: 24074220

95. Kotera Y, Hangai M, Hirose F, Mori S, Yoshimura N. Three-Dimensional Imaging of Macular Inner Structures in Glaucoma by Using Spectral-Domain Optical Coherence Tomography. Investig Opthalmology Vis Sci. 2011; 52: 1412. https://doi.org/10.1167/iovs.10-5572 PMID: 21087959

96. Kotowski J, Folio LS, Wollstein G, Ishikawa H, Ling Y, Bilonick RA, et al. Glaucoma discrimination of segmented cirrus spectral domain optical coherence tomography (SD-OCT) macular scans. Br J Ophthalmol. 2012; 96: 1420–1425. https://doi.org/10.1136/bjophthalmol-2011-301021 PMID: 22914498

97. Larrosa JM, Polo V, Ferreras A, García-Martín E, Calvo P, Pablo LE. Neural Network Analysis of Different Segmentation Strategies of Nerve Fiber Layer Assessment for Glaucoma Diagnosis: J Glaucoma. 2015; 24: 672–678. https://doi.org/10.1097/IJG.0000000000000071 PMID: 25055209

98. Lee EJ, Lee KM, Kim H, Kim T-W. Glaucoma Diagnostic Ability of the New Circumpapillary Retinal Nerve Fiber Layer Thickness Analysis Based on Bruch's Membrane Opening. Investig Opthalmology Vis Sci. 2016; 57: 4194. https://doi.org/10.1167/iovs.16-19578 PMID: 27548890

99. Lee KM, Lee EJ, Kim T-W, Kim H. Comparison of the Abilities of SD-OCT and SS-OCT in Evaluating the Thickness of the Macular Inner Retinal Layer for Glaucoma Diagnosis. Gonzalez P, editor. PLOS ONE. 2016; 11: e0147964. https://doi.org/10.1371/journal.pone.0147964 PMID: 26812064

100. Lee S, Sung KR, Cho JW, Cheon MH, Kang SY, Kook MS. Spectral-domain optical coherence tomography and scanning laser polarimetry in glaucoma diagnosis. Jpn J Ophthalmol. 2010; 54: 544–549. https://doi.org/10.1007/s10384-010-0870-5 PMID: 21191714

101. Leite MT, Rao HL, Zangwill LM, Weinreb RN, Medeiros FA. Comparison of the Diagnostic Accuracies of the Spectralis, Cirrus, and RTVue Optical Coherence Tomography Devices in Glaucoma. Ophthalmology. 2011; https://doi.org/10.1016/j.ophtha.2010.11.029 PMID: 21377735

102. Leite MT, Zangwill LM, Weinreb RN, Rao HL, Alencar LM, Sample PA, et al. Effect of disease severity on the performance of Cirrus spectral-domain OCT for glaucoma diagnosis. Invest Ophthalmol Vis Sci. 2010; 51: 4104–4109. https://doi.org/10.1167/iovs.09-4716 PMID: 20335619

103. Leung CK, Chan W, Chong KK-L, Yung W, Tang K, Woo J, et al. Comparative Study of Retinal Nerve Fiber Layer Measurement by StratusOCT and GDx VCC, I: Correlation Analysis in Glaucoma. Investig Opthalmology Vis Sci. 2005; 46: 3214. https://doi.org/10.1167/iovs.05-0294 PMID: 16123421

104. Leung CK, Chan W, Hui Y, Yung W, Woo J, Tsang M, et al. Analysis of Retinal Nerve Fiber Layer and Optic Nerve Head in Glaucoma with Different Reference Plane Offsets, Using Optical Coherence

Tomography. Investig Opthalmology Vis Sci. 2005; 46: 891. https://doi.org/10.1167/iovs.04-1107 PMID: 15728545

105. Leung CK, Cheung CY, Weinreb RN, Qiu Q, Liu S, Li H, et al. Retinal Nerve Fiber Layer Imaging with Spectral-Domain Optical Coherence Tomography. Ophthalmology. 2009; 116: 1257–1263.e2. https://doi.org/10.1016/j.ophtha.2009.04.013 PMID: 19464061

106. Leung CK, Ye C, Weinreb RN, Cheung CYL, Qiu Q, Liu S, et al. Retinal Nerve Fiber Layer Imaging with Spectral-Domain Optical Coherence Tomography. Ophthalmology. 2010; 117: 267–274. https://doi.org/10.1016/j.ophtha.2009.06.061 PMID: 19969364

107. Leung CKS, Lam S, Weinreb RN, Liu S, Ye C, Liu L, et al. Retinal Nerve Fiber Layer Imaging with Spectral-Domain Optical Coherence Tomography. Ophthalmology. 2010; 117: 1684–1691. https://doi.org/10.1016/j.ophtha.2010.01.026 PMID: 20663563

108. Lisboa R, Leite MT, Zangwill LM, Tafreshi A, Weinreb RN, Medeiros FA. Diagnosing Preperimetric Glaucoma with Spectral Domain Optical Coherence Tomography. Ophthalmology. 2012; 119: 2261–2269. https://doi.org/10.1016/j.ophtha.2012.06.009 PMID: 22883689

109. Lisboa R, Leite MT, Zangwill LM, Tafreshi A, Weinreb RN, Medeiros FA. Diagnosing Preperimetric Glaucoma with Spectral Domain Optical Coherence Tomography. Ophthalmology. 2012; 119: 2261–2269. https://doi.org/10.1016/j.ophtha.2012.06.009 PMID: 22883689

110. Liu S, Wang B, Yin B, Milner TE, Markey MK, McKinnon SJ, et al. Retinal Nerve Fiber Layer Reflectance for Early Glaucoma Diagnosis: J Glaucoma. 2014; 23: e45–e52. https://doi.org/10.1097/IJG.0b013e31829ea2a7 PMID: 23835671

111. Lu AT-H, Wang M, Varma R, Schuman JS, Greenfield DS, Smith SD, et al. Combining Nerve Fiber Layer Parameters to Optimize Glaucoma Diagnosis with Optical Coherence Tomography. Ophthalmology. 2008; 115: 1352–1357.e2. https://doi.org/10.1016/j.ophtha.2008.01.011 PMID: 18514318

112. Medeiros FA, Lisboa R, Weinreb RN, Girkin CA, Liebmann JM, Zangwill LM. A Combined Index of Structure and Function for Staging Glaucomatous Damage. Arch Ophthalmol. 2012; 130. https://doi.org/10.1001/archophthalmol.2012.827 PMID: 23130365

113. Medeiros FA, Zangwill LM, Bowd C, Weinreb RN. Comparison of the GDx VCC scanning laser polarimeter, HRT II confocal scanning laser ophthalmoscope, and stratus OCT optical coherence tomograph for the detection of glaucoma. Arch Ophthalmol Chic Ill 1960. 2004; 122: 827–837. https://doi.org/10.1001/archopht.122.6.827 PMID: 15197057

114. Mendez-Hernandez C, Rodriguez-Uña I, Gonzalez-de-la Rosa M, Arribas-Pardo P, Garcia-Feijoo J. Glaucoma diagnostic capacity of optic nerve head haemoglobin measures compared with spectral domain OCT and HRT III confocal tomography. Acta Ophthalmol (Copenh). 2016; 94: 697–704. https://doi.org/10.1111/aos.13050 PMID: 27130650

115. Monsalve B, Ferreras A, Calvo P, Urcola JA, Figus M, Monsalve J, et al. Diagnostic ability of Humphrey perimetry, Octopus perimetry, and optical coherence tomography for glaucomatous optic neuropathy. Eye. 2016; https://doi.org/10.1038/eye.2016.251 PMID: 27834960

116. Moreno-Montañés J, Antón A, García N, Olmo N, Morilla A, Fallon M. Comparison of Retinal Nerve Fiber Layer Thickness Values Using Stratus Optical Coherence Tomography and Heidelberg Retina Tomograph-III: J Glaucoma. 2009; 18: 528–534. https://doi.org/10.1097/IJG.0b013e318193c29f PMID: 19745667

117. Moreno-Montañés J, Olmo N, Alvarez A, García N, Zarranz-Ventura J. Cirrus High-Definition Optical Coherence Tomography Compared with Stratus Optical Coherence Tomography in Glaucoma Diagnosis. Investig Opthalmology Vis Sci. 2010; 51: 335. https://doi.org/10.1167/iovs.08-2988 PMID: 19737881

118. Na JH, Lee K, Lee JR, Baek S, Yoo SJ, Kook MS. Detection of macular ganglion cell loss in preperimetric glaucoma patients with localized retinal nerve fibre defects by spectral-domain optical coherence tomography: Detection of ganglion cell complex loss in preperimetric glaucoma. Clin Experiment Ophthalmol. 2013; 41: 870–880. https://doi.org/10.1111/ceo.12142 PMID: 23777476

119. Na JH, Lee KS, Lee JR, Lee Y, Kook MS. The glaucoma detection capability of spectral-domain OCT and GDx-VCC deviation maps in early glaucoma patients with localized visual field defects. Graefes Arch Clin Exp Ophthalmol. 2013; 251: 2371–2382. https://doi.org/10.1007/s00417-013-2362-z PMID: 23818227

120. Na JH, Sung KR, Baek S, Kim YJ, Durbin MK, Lee HJ, et al. Detection of Glaucoma Progression by Assessment of Segmented Macular Thickness Data Obtained Using Spectral Domain Optical Coherence Tomography. Investig Opthalmology Vis Sci. 2012; 53: 3817. https://doi.org/10.1167/iovs.11-9369 PMID: 22562510

121. Na JH, Sung KR, Baek S, Sun JH, Lee Y. Macular and Retinal Nerve Fiber Layer Thickness: Which Is More Helpful in the Diagnosis of Glaucoma? Investig Opthalmology Vis Sci. 2011; 52: 8094. https://doi.org/10.1167/iovs.11-7833 PMID: 21911590

122. Nakatani Y, Higashide T, Ohkubo S, Sugiyama K. Influences of the Inner Retinal Sublayers and Analytical Areas in Macular Scans by Spectral-Domain OCT on the Diagnostic Ability of Early Glaucoma. Investig Opthalmology Vis Sci. 2014; 55: 7479. https://doi.org/10.1167/iovs.14-15530 PMID: 25342613

123. Nomoto H, Matsumoto C, Takada S, Hashimoto S, Arimura E, Okuyama S, et al. Detectability of glaucomatous changes using SAP, FDT, flicker perimetry, and OCT. J Glaucoma. 2009; 18: 165–171. https://doi.org/10.1097/IJG.0b013e318179f7ca PMID: 19225357

124. Nouri-Mahdavi K, Nowroozizadeh S, Nassiri N, Cirineo N, Knipping S, Giaconi J, et al. Macular Ganglion Cell/Inner Plexiform Layer Measurements by Spectral Domain Optical Coherence Tomography for Detection of Early Glaucoma and Comparison to Retinal Nerve Fiber Layer Measurements. Am J Ophthalmol. 2013; 156: 1297–1307.e2. https://doi.org/10.1016/j.ajo.2013.08.001 PMID: 24075422

125. Oli A, Joshi D. Can ganglion cell complex assessment on cirrus HD OCT aid in detection of early glaucoma? Saudi J Ophthalmol. 2015; 29: 201–204. https://doi.org/10.1016/j.sjopt.2015.02.007 PMID: 26155079

126. Pablo LE, Ferreras A, Schlottmann PG. Retinal nerve fibre layer evaluation in ocular hypertensive eyes using optical coherence tomography and scanning laser polarimetry in the diagnosis of early glaucomatous defects. Br J Ophthalmol. 2011; 95: 51–55. https://doi.org/10.1136/bjo.2009.170936 PMID: 20576777

127. Parikh RS, Parikh S, Sekhar GC, Kumar RS, Prabakaran S, Ganesh Babu J, et al. Diagnostic Capability of Optical Coherence Tomography (Stratus OCT 3) in Early Glaucoma. Ophthalmology. 2007; 114: 2238–2243. https://doi.org/10.1016/j.ophtha.2007.03.005 PMID: 17561260

128. Parikh RS, Parikh SR, Thomas R. Diagnostic capability of macular parameters of Stratus OCT 3 in detection of early glaucoma. Br J Ophthalmol. 2010; 94: 197–201. https://doi.org/10.1136/bjo.2008.143602 PMID: 19493860

129. Park HYL, Park CK. Structure-Function Relationship and Diagnostic Value of RNFL Area Index Compared With Circumpapillary RNFL Thickness by Spectral-Domain OCT: J Glaucoma. 2013; 22: 88–97. https://doi.org/10.1097/IJG.0b013e318231202f PMID: 23232911

130. Park H-YL, Park CK. Diagnostic Capability of Lamina Cribrosa Thickness by Enhanced Depth Imaging and Factors Affecting Thickness in Patients with Glaucoma. Ophthalmology. 2013; 120: 745–752. https://doi.org/10.1016/j.ophtha.2012.09.051 PMID: 23260259

131. Park J-W, Jung H-H, Heo H, Park S-W. Validity of the temporal-to-nasal macular ganglion cell-inner plexiform layer thickness ratio as a diagnostic parameter in early glaucoma. Acta Ophthalmol (Copenh). 2015; 93: e356–e365. https://doi.org/10.1111/aos.12666 PMID: 25619801

132. Park SB, Sung KR, Kang SY, Kim KR, Kook MS. Comparison of glaucoma diagnostic capabilities of Cirrus HD and Stratus optical coherence tomography. Arch Ophthalmol. 2009; 127: 1603–1609. https://doi.org/10.1001/archophthalmol.2009.296 PMID: 20008715

133. Pueyo V, Polo V, Larrosa JM, Ferreras A, Pablo LE, Honrubia FM. Diagnostic ability of the Heidelberg retina tomograph, optical coherence tomograph, and scanning laser polarimeter in open-angle glaucoma. J Glaucoma. 2007; 16: 173–177. https://doi.org/10.1097/IJG.0b013e31802dfc1d PMID: 17473725

134. Rao HL, Addepalli UK, Chaudhary S, Kumbar T, Senthil S, Choudhari NS, et al. Ability of Different Scanning Protocols of Spectral Domain Optical Coherence Tomography to Diagnose Preperimetric GlaucomaDiagnostic Ability of SDOCT in Preperimetric Glaucoma. Invest Ophthalmol Vis Sci. 2013; 54: 7252–7257. https://doi.org/10.1167/iovs.13-12731 PMID: 24114539

135. Rao HL, Kumbar T, Addepalli UK, Bharti N, Senthil S, Choudhari NS, et al. Effect of Spectrum Bias on the Diagnostic Accuracy of Spectral-Domain Optical Coherence Tomography in Glaucoma. Investig Opthalmology Vis Sci. 2012; 53: 1058. https://doi.org/10.1167/iovs.11-8463 PMID: 22266520

136. Rao HL, Yadav RK, Addepalli UK, Begum VU, Senthil S, Choudhari NS, et al. Reference Standard Test and the Diagnostic Ability of Spectral Domain Optical Coherence Tomography in Glaucoma: J Glaucoma. 2015; 24: e151–e156. https://doi.org/10.1097/IJG.0000000000000087 PMID: 25014362

137. Rao HL, Yadav RK, Addepalli UK, Chaudhary S, Senthil S, Choudhari NS, et al. Peripapillary Retinal Nerve Fiber Layer Assessment of Spectral Domain Optical Coherence Tomography and Scanning Laser Polarimetry to Diagnose Preperimetric Glaucoma. Bhattacharya S, editor. PLoS ONE. 2014; 9: e108992. https://doi.org/10.1371/journal.pone.0108992 PMID: 25279801

138. Rao HL, Zangwill LM, Weinreb RN, Sample PA, Alencar LM, Medeiros FA. Comparison of Different Spectral Domain Optical Coherence Tomography Scanning Areas for Glaucoma Diagnosis. Ophthalmology. 2010; 117: 1692–1699.e1. https://doi.org/10.1016/j.ophtha.2010.01.031 PMID: 20493529

139. Rao HL, Babu JG, Addepalli UK, Senthil S, Garudadri CS. Retinal nerve fiber layer and macular inner retina measurements by spectral domain optical coherence tomograph in Indian eyes with early glaucoma. Eye. 2012; 26: 133–139. https://doi.org/10.1038/eye.2011.277 PMID: 22079964

140. Rao HL, Yadav RK, Addepalli UK, Chaudhary S, Senthil S, Choudhari NS, et al. Retinal nerve fiber layer evaluation of spectral domain optical coherence tomograph and scanning laser polarimeter to diagnose glaucoma. Eye. 2014; 28: 654–661. https://doi.org/10.1038/eye.2014.46 PMID: 24603422

141. Raza AS, Zhang X, De Moraes CGV, Reisman CA, Liebmann JM, Ritch R, et al. Improving Glaucoma Detection Using Spatially Correspondent Clusters of Damage and by Combining Standard Automated Perimetry and Optical Coherence Tomography. Investig Opthalmology Vis Sci. 2014; 55: 612. https://doi.org/10.1167/iovs.13-12351 PMID: 24408977

142. Rimayanti U, Latief MA, Arintawati P, Akita T, Tanaka J, Kiuchi Y. Width of abnormal ganglion cell complex area determined using optical coherence tomography to predict glaucoma. Jpn J Ophthalmol. 2014; 58: 47–55. https://doi.org/10.1007/s10384-013-0281-5 PMID: 24150101

143. Rolle T, Manerba L, Lanzafame P, Grignolo FM. Diagnostic Power of Macular Retinal Thickness Analysis and Structure-Function Relationship in Glaucoma Diagnosis Using SPECTRALIS OCT. Curr Eye Res. 2015; 1–9. https://doi.org/10.3109/02713683.2015.1043134 PMID: 26200743

144. Rolle T. Ganglion cell complex and retinal nerve fiber layer measured by fourier-domain optical coherence tomography for early detection of structural damage in patients with preperimetric glaucoma. Clin Ophthalmol. 2011; 961. https://doi.org/10.2147/OPTH.S20249 PMID: 21792286

145. Schrems WA, Mardin CY, Horn FK, Juenemann AGM, Laemmer R. Comparison of Scanning Laser Polarimetry and Optical Coherence Tomography in Quantitative Retinal Nerve Fiber Assessment: J Glaucoma. 2010; 19: 83–94. https://doi.org/10.1097/IJG.0b013e3181a2fc0e PMID: 19373100

146. Schulze A, Lamparter J, Pfeiffer N, Berisha F, Schmidtmann I, Hoffmann EM. Diagnostic ability of retinal ganglion cell complex, retinal nerve fiber layer, and optic nerve head measurements by Fourier-domain optical coherence tomography. Graefes Arch Clin Exp Ophthalmol. 2011; 249: 1039–1045. https://doi.org/10.1007/s00417-010-1585-5 PMID: 21240522

147. Schulze A, Lamparter J, Pfeiffer N, Berisha F, Schmidtmann I, Hoffmann EM. Comparison of Laser Scanning Diagnostic Devices for Early Glaucoma Detection: J Glaucoma. 2015; 24: 442–447. https://doi.org/10.1097/IJG.0000000000000054 PMID: 24844535

148. Sehi M, Grewal DS, Sheets CW, Greenfield DS. Diagnostic Ability of Fourier-Domain vs Time-Domain Optical Coherence Tomography for Glaucoma Detection. Am J Ophthalmol. 2009; 148: 597–605. https://doi.org/10.1016/j.ajo.2009.05.030 PMID: 19589493

149. Sevim MS, Buttanri B, Acar BT, Kahya A, Vural ET, Acar S. Ability of Fourier-domain Optical Coherence Tomography to Detect Retinal Ganglion Cell Complex Atrophy in Glaucoma Patients: J Glaucoma. 2013; 22: 542–549. https://doi.org/10.1097/IJG.0b013e31824d1f97 PMID: 22407395

150. Shah SB, Garcia AG, Leiby BE, Cox LA, Katz LJ, Myers JS. Color Reflectivity Discretization Analysis of OCT Images in the Detection of Glaucomatous Nerve Fiber Layer Defects: J Glaucoma. 2016; 25: e346–e354. https://doi.org/10.1097/IJG.0000000000000363 PMID: 26766397

151. Shieh E, Lee R, Que C, Srinivasan V, Guo R, DeLuna R, et al. Diagnostic Performance of a Novel Three-Dimensional Neuroretinal Rim Parameter for Glaucoma Using High-Density Volume Scans. Am J Ophthalmol. 2016; 169: 168–178. https://doi.org/10.1016/j.ajo.2016.06.028 PMID: 27349414

152. Shin CJ, Sung KR, Um TW, Kim YJ, Kang SY, Cho JW, et al. Comparison of retinal nerve fibre layer thickness measurements calculated by the optic nerve head map (NHM4) and RNFL3.45 modes of spectral-domain optical coherence tomography (RTVue-100). Br J Ophthalmol. 2010; 94: 763–767. https://doi.org/10.1136/bjo.2009.166314 PMID: 20508052

153. Shin H-Y, Park H-YL, Jung K-I, Choi J-A, Park CK. Glaucoma Diagnostic Ability of Ganglion Cell–Inner Plexiform Layer Thickness Differs According to the Location of Visual Field Loss. Ophthalmology. 2014; 121: 93–99. https://doi.org/10.1016/j.ophtha.2013.06.041 PMID: 23962652

154. Shin HY, Park H-YL, Jung KI, Park CK. Glaucoma diagnosis optic disc analysis comparing Cirrus spectral domain optical coherence tomography and Heidelberg retina tomograph II. Jpn J Ophthalmol. 2013; 57: 41–46. https://doi.org/10.1007/s10384-012-0205-9 PMID: 23104685

155. Shin HJ, Cho BJ. Comparison of Retinal Nerve Fiber Layer Thickness between Stratus and Spectralis OCT. Korean J Ophthalmol. 2011; 25: 166. https://doi.org/10.3341/kjo.2011.25.3.166 PMID: 21655041

156. Shin JW, Uhm KB, Seong M. Retinal Nerve Fiber Layer Defect Volume Deviation Analysis Using Spectral-Domain Optical Coherence TomographyRNFL Defect Volume Deviation Analysis. Invest Ophthalmol Vis Sci. 2015; 56: 21–28.

157. Shoji T, Nagaoka Y, Sato H, Chihara E. Impact of high myopia on the performance of SD-OCT parameters to detect glaucoma. Graefes Arch Clin Exp Ophthalmol. 2012; 250: 1843–1849. https://doi.org/10.1007/s00417-012-1994-8 PMID: 22555896

158. Silva FR, Vidotti VG, Cremasco F, Dias M, Gomi ES, Costa VP. Sensitivity and specificity of machine learning classifiers for glaucoma diagnosis using Spectral Domain OCT and standard automated perimetry. Arq Bras Oftalmol. 2013; 76: 170–174. PMID: 23929078

159. Simavli H, Que CJ, Akduman M, Rizzo JL, Tsikata E, de Boer JF, et al. Diagnostic Capability of Peripapillary Retinal Thickness in Glaucoma Using 3D Volume Scans. Am J Ophthalmol. 2015; 159: 545–556.e2. https://doi.org/10.1016/j.ajo.2014.12.004 PMID: 25498354

160. Suh MH, Kim SK, Park KH, Kim DM, Kim SH, Kim HC. Combination of optic disc rim area and retinal nerve fiber layer thickness for early glaucoma detection by using spectral domain OCT. Graefes Arch Clin Exp Ophthalmol. 2013; 251: 2617–2625. https://doi.org/10.1007/s00417-013-2468-3 PMID: 24065214

161. Sullivan-Mee M, Ruegg CC, Pensyl D, Halverson K, Qualls C. Diagnostic Precision of Retinal Nerve Fiber Layer and Macular Thickness Asymmetry Parameters for Identifying Early Primary Open-Angle Glaucoma. Am J Ophthalmol. 2013; 156: 567–577.e1. https://doi.org/10.1016/j.ajo.2013.04.037 PMID: 23810475

162. Sung KR, Na JH, Lee Y. Glaucoma Diagnostic Capabilities of Optic Nerve Head Parameters as Determined by Cirrus HD Optical Coherence Tomography: J Glaucoma. 2012; 21: 498–504. https://doi.org/10.1097/IJG.0b013e318220dbb7 PMID: 21637115

163. Sung M-S, Kang B-W, Kim H-G, Heo H, Park S-W. Clinical Validity of Macular Ganglion Cell Complex by Spectral Domain-Optical Coherence Tomography in Advanced Glaucoma: J Glaucoma. 2014; 23: 341–346. https://doi.org/10.1097/IJG.0b013e318279c932 PMID: 23221905

164. Sung MS, Yoon JH, Heo H, Park SW. Effect of myopic refractive error on the glaucoma diagnostic ability of cirrus high-definition optical coherence tomography. Acta Ophthalmol (Copenh). 2015; 93: e236–e237. https://doi.org/10.1111/aos.12546 PMID: 25175669

165. Sung M-S, Yoon J-H, Park S-W. Diagnostic Validity of Macular Ganglion Cell-Inner Plexiform Layer Thickness Deviation Map Algorithm Using Cirrus HD-OCT in Preperimetric and Early Glaucoma: J Glaucoma. 2014; 23: e144–e151. https://doi.org/10.1097/IJG.0000000000000028 PMID: 24240879

166. Takayama K, Hangai M, Durbin M, Nakano N, Morooka S, Akagi T, et al. A Novel Method to Detect Local Ganglion Cell Loss in Early Glaucoma Using Spectral-Domain Optical Coherence Tomography. Investig Opthalmology Vis Sci. 2012; 53: 6904. https://doi.org/10.1167/iovs.12-10210 PMID: 22977136

167. Toshev AP, Lamparter J, Pfeiffer N, Hoffmann EM. Bruch's Membrane Opening-Minimum Rim Width Assessment With Spectral-Domain Optical Coherence Tomography Performs Better Than Confocal Scanning Laser Ophthalmoscopy in Discriminating Early Glaucoma Patients From Control Subjects: J Glaucoma. 2017; 26: 27–33. https://doi.org/10.1097/IJG.0000000000000532 PMID: 27636592

168. Ulas F, Dogan Ü, Kaymaz A, Çelik F, Çelebi S. Evaluation of subjects with a moderate cup to disc ratio using optical coherence tomography and Heidelberg retina tomograph 3: Impact of the disc area. Indian J Ophthalmol. 2015; 63: 3. https://doi.org/10.4103/0301-4738.151454 PMID: 25686054

169. Vessani RM, Moritz R, Batis L, Zagui RB, Bernardoni S, Susanna R. Comparison of quantitative imaging devices and subjective optic nerve head assessment by general ophthalmologists to differentiate normal from glaucomatous eyes. J Glaucoma. 2009; 18: 253–261. https://doi.org/10.1097/IJG.0b013e31818153da PMID: 19295383

170. Wang M, Lu AT-H, Varma R, Schuman JS, Greenfield DS, Huang D. Combining Information From 3 Anatomic Regions in the Diagnosis of Glaucoma With Time-Domain Optical Coherence Tomography: J Glaucoma. 2014; 23: 129–135. https://doi.org/10.1097/IJG.0b013e318264b941 PMID: 22828002

171. Wang X, Li S, Fu J, Wu G, Mu D, Li S, et al. Comparative study of retinal nerve fibre layer measurement by RTVue OCT and GDx VCC. Br J Ophthalmol. 2011; 95: 509–513. https://doi.org/10.1136/bjo.2009.163493 PMID: 20657017

172. Wollstein G, Ishikawa H, Wang J, Beaton SA, Schuman JS. Comparison of three optical coherence tomography scanning areas for detection of glaucomatous damage. Am J Ophthalmol. 2005; 139: 39–43. https://doi.org/10.1016/j.ajo.2004.08.036 PMID: 15652826

173. Wu H, de Boer JF, Chen TC. Diagnostic Capability of Spectral-Domain Optical Coherence Tomography for Glaucoma. Am J Ophthalmol. 2012; 153: 815–826.e2. https://doi.org/10.1016/j.ajo.2011.09.032 PMID: 22265147

174. Yang Z, Tatham AJ, Weinreb RN, Medeiros FA, Liu T, Zangwill LM. Diagnostic Ability of Macular Ganglion Cell Inner Plexiform Layer Measurements in Glaucoma Using Swept Source and Spectral Domain Optical Coherence Tomography. Linden R, editor. PLOS ONE. 2015; 10: e0125957. https://doi.org/10.1371/journal.pone.0125957 PMID: 25978420

175. Yoon MH, Park SJ, Kim CY, Chin HS, Kim NR. Glaucoma diagnostic value of the total macular thickness and ganglion cell-inner plexiform layer thickness according to optic disc area. Br J Ophthalmol. 2014; 98: 315–321. https://doi.org/10.1136/bjophthalmol-2013-303185 PMID: 24385290

176. Zhang Y, Wen W, Sun X. Comparison of Several Parameters in Two Optical Coherence Tomography Systems for Detecting Glaucomatous Defects in High Myopia. Investig Opthalmology Vis Sci. 2016; 57: 4910. https://doi.org/10.1167/iovs.16-19104 PMID: 27654417

177. Zhong Y, Shen X, Zhou X, Cheng Y, Min Y. Blue-on-yellow perimetry and optical coherence tomography in patients with preperimetric glaucoma. Clin Experiment Ophthalmol. 2009; 37: 262–269. https://doi.org/10.1111/j.1442-9071.2009.02031.x PMID: 19472535

178. Zhong Y, Zhou X, Cheng Y, Xie L. Relation between blue-on-yellow perimetry and optical coherence tomography in normal tension glaucoma. Can J Ophthalmol Can Ophtalmol. 2010; 45: 494–500.

179. Traynis I, De Moraes CG, Raza AS, Liebmann JM, Ritch R, Hood DC. Prevalence and Nature of Early Glaucomatous Defects in the Central 10˚ of the Visual Field. JAMA Ophthalmol. 2014; 132: 291. https://doi.org/10.1001/jamaophthalmol.2013.7656 PMID: 24407153

180. Mazzarella J, Cole J. The anatomy of an OCT scan. Rev Optom. 2015; 152.9: 58.

181. Michelessi M, Lucenteforte E, Oddone F, Brazzelli M, Parravano M, Franchi S, et al. Optic nerve head and fibre layer imaging for diagnosing glaucoma. In: The Cochrane Collaboration, editor. Cochrane Database of Systematic Reviews. Chichester, UK: John Wiley & Sons, Ltd; 2015. https://doi.org/10.1002/14651858.CD008803.pub2 PMID: 26618332

182. Ahmed S, Khan Z, Si F, Mao A, Pan I, Yazdi F, et al. Summary of Glaucoma Diagnostic Testing Accuracy: An Evidence-Based Meta-Analysis. J Clin Med Res. 2016; 8: 641–649. https://doi.org/10.14740/jocmr2643w PMID: 27540437

183. Oddone F, Lucenteforte E, Michelessi M, Rizzo S, Donati S, Parravano M, et al. Macular versus Retinal Nerve Fiber Layer Parameters for Diagnosing Manifest Glaucoma. Ophthalmology. 2016; 123: 939–949. https://doi.org/10.1016/j.ophtha.2015.12.041 PMID: 26891880

184. Chen H-Y, Chang Y-C. Meta-analysis of stratus OCT glaucoma diagnostic accuracy. Optom Vis Sci. 2014; 91: 1129–1139. https://doi.org/10.1097/OPX.0000000000000331 PMID: 25036543

185. Fallon M, Valero O, Pazos M, Antón A. Diagnostic Accuracy of Imaging Devices in Glaucoma: A Meta-Analysis. Surv Ophthalmol. 2017; https://doi.org/10.1016/j.survophthal.2017.01.001 PMID: 28093287

186. Whiting P, Rutjes AWS, Dinnes J, Reitsma J, Bossuyt PMM, Kleijnen J. Development and validation of methods for assessing the quality of diagnostic accuracy studies. Health Technol Assess Winch Engl. 2004; 8: iii, 1–234.